Quality control of the quality control: Improving the understanding of analytical separation techniques for the assessment of mRNA integrity in a biotherapeutic context.

Jessica Tran

A thesis submitted to the University of Ottawa in partial fulfillment of the requirements for the
Master's degree in Biochemistry

Department of Biochemistry, Microbiology, and Immunology
Faculty of Medicine
University of Ottawa

Abstract

Despite the growing interest in mRNA-based therapeutics, the platform's novelty, and lack of published knowledge regarding mRNA quality attributes and assessment pose significant challenges in establishing guidelines and references for therapeutic mRNA analysis. As bioassays and *in vitro* translation assays are yet to be widely accepted to assess efficacy, physicochemical assays such as capillary electrophoresis and ion-pair reversed phase liquid chromatography serve as surrogates for quality assurance by measuring transcript length. While both are accepted bioanalytical techniques to assess transcript length, we reveal that they are not interchangeable and have significant resolution differences. In this work, we demonstrate how various factors such as method parameters, product-specific sample preparation, and excipients can easily influence mRNA integrity measurements. We emphasize the importance of understanding the influence of method parameters on mRNA integrity assessment and impurity detection by capillary gel electrophoresis and ion-pair reversed phase liquid chromatography, especially in a biotherapeutic context where mRNA is modified and encapsulated. Such knowledge is imperative in making accurate comparisons between mRNA products and designing practical reference standards.

We anticipate that this work will be valuable for not only biopharmaceutical professionals but also for regulatory bodies. By providing insight into the performance of different analytical methods for assessing mRNA integrity, our study can facilitate the development of more optimized analytical methods and contribute to the overall quality assurance of mRNA-based therapies.

Acknowledgements

First, I must thank my supervisor Dr. Huixin (Lulu) Lu. I'll never find the words to truly express the extent of my gratitude and appreciation for you as both a mentor and a person, but I can try. You always gently (yet consistently) nudge me out of my comfort zone and throw ideas at me – allowing me to explore and grow as a scientist. I seriously would not be here without your mentorship and guidance over the past few years. My co-supervisors, Dr. Sean Li, and Dr. Lisheng Wang, thank you both for your constant encouragement and excellent insights. I'd also like to thank my committee, Dr. Christopher Boddy and Dr. Michel Girard. I'm extremely grateful to have such a brilliant team of scientists in my corner.

I must also acknowledge all my wonderful colleagues, new and old, in the Separation Science Lab, and the Regulatory Research Division. Thank you for all your help and unwavering support over the years. I feel extremely fortunate to be able to work with such amazing people who share the same passion for science. Of course, I have to thank Dr. Simon Sauvé for the giving me the opportunity to work with such wonderful scientists in the first place. Thank you for giving a chance to a completely inexperienced undergraduate student.

To my family and friends outside of science, thank you for always listening to my endless rambling even though I'm sure it all sounded like gibberish to you. Thank you to my circus of friends for all your constant support and for keeping me sane with all your insanity.

Table of Contents

Abstract ii
Acknowledgements iii
Table of Contents iv
List of Abbreviations viii
List of Tables x
List of Figures xi
1 Introduction 1
1.1 mRNA Vaccines and Therapeutics 1
1.1.1 Structure of mRNA vaccines 1
1.1.2 Mechanism of action 4
1.1.3 General manufacturing process 5
1.1.4 Lipid nanoparticles delivery system 7
1.2 Current Regulatory Guidelines and the Need for Standardization 9
1.2.1 mRNA vaccine impurities and critical quality attributes 10
1.3 Analytical Methods Used for the Assessment of mRNA Integrity 11
1.3.1 Capillary gel electrophoresis 12
1.3.2 Ion-pair reversed-phase liquid chromatography 12
1.4 Research Objectives 13
2 Comparative analysis of commercial and in-house capillary gel electrophoresis for RNA separation 16
2.1 Background 16
2.2 Materials and Methods 17
2.2.1 Reagents and samples 17
2.2.2 Sample preparation for CGE-LIF analysis 18
2.2.3 Instrumentation 18
2.2.4 Commercial CGE-LIF RNA analysis kit 18
2.2.5 In-house CGE-LIF method parameters and analysis 19
2.2.6 Agarose gel electrophoresis 19
2.2.7 IP-RP HPLC 20
2.3 Results and Discussion 20

2.3.1 Head-to-head comparison of commercial kit and in-house CGE method for separation of RNA ladders 20
2.3.2 Investigation of RNA ladder misalignment 27
2.4 Conclusion 29
3 A comprehensive evaluation of method parameters critical to the reliable assessment of therapeutic mRNA integrity by capillary gel electrophoresis 31
3.1 Background 31
3.2 Materials and Methods 31
3.2.1 Reagents and samples 31
3.2.2 Lipid nanoparticle disruption and sample preparation 32
3.2.3 AGE 32
3.2.4 CGE-LIF instrumentation 32
3.2.5 CGE-LIF analysis 33
3.2.6 DOE set up and data analysis 33
3.3 Results and Discussion 34
3.3.1 Effect of denaturants and gel additives on the separation of RNA by CGE-LIF in one-factor at a time experiments 34
3.3.2 Separation of mRNA-LNP samples and quantification of disruption efficiency 38
3.3.3 Design of experiments approach to systematically evaluate interactive effects of method parameters that influence CGE-LIF method performance 41
3.4 Conclusion 45
4 A comparative analysis of capillary gel electrophoresis and ion-pair reversed phase liquid chromatography for the assessment of mRNA therapeutics 47
4.1 Background 47
4.2 Materials and Methods 47
4.2.1 Reagents and samples 47
4.2.2 LNP disruption and sample preparation 48
4.2.3 Instrumentation 48
4.2.4 CGE-LIF analysis 48
4.2.5 IP-RP HPLC 48
4.2.6 Electropherogram integration and data analysis 49
4.3 Results and Discussion 49
4.3.1 Evaluation of method performance 49
4.3.2 Integrity analysis of mRNA-LNP samples 51

4.4 Conclusion 53
5 Protection of mRNA payloads by LNP and the thermal stability of mRNA-LNP 55
5.1 Background 55
5.2 Materials and Methods 56
5.2.1 Reagents and samples 56
5.2.2 LNP disruption and thermal stability study 56
5.2.3 CGE-LIF instrumentation 57
5.2.4 CGE-LIF analysis 57
5.2.5 Electropherogram integration and data analysis 57
5.3 Results and Discussion 57
5.3.1 Protective effect of LNP on mRNA 57
5.3.2 Thermal stability of mRNA extracted from LNP over time 59
6 Conclusion 61
7 References 63
8 Contributions of Collaborators 70
9 Appendices 71
9.1 Electropherogram integration example 71
9.2 Appendix A: Calculation of resolution factor (R_s) 71

List of Abbreviations

AGE	Agarose gel electrophoresis
AmAc	Ammonium acetate
bp	Base pair
BRDD	Biologic and Radiopharmaceutical Drugs Directorate
CGE	Capillary gel electrophoresis
CQA	Critical quality attribute
DBAA	Dibutylammonium acetate
DEPC	Diethyl pyrocarbonate
DMGPEG-2000	1,2-dimyristoyl-rac-glycero-3-methoxypolyethylene glycol-2000
DNA	Deoxyribonucleic acid
DOE	Design of experiments
DP	Drug product
DPSC	Diasteroylphosphatidylcholine
DS	Drug substance
EDTA	Ethylenediaminetetraacetic acid
EMA	European Medicines Agency
EtOH	Ethanol
FLuc	Firefly luciferase
GLM	General linear model
HC	Health Canada
HCl	Hydrochloric acid
HPFB	Health Products and Food Branch

HPLC	High performance liquid chromatography
IPA	Isopropanol
IP-RPLC	Ion pair reversed phase liquid chromatography
IST	Internal standard
IVT	In vitro transcribed
LIF	Laser induced fluorescence
LNP	Lipid nanoparticles
MeOH	Methanol
mRNA	Messenger ribonucleic acid
MW	Molecular weight
NaOH	Sodium hydroxide
NEB	New England Biolabs
NFW	Nuclease-free water
nt	Nucleotide
PDA	Photodiode array
PEG	Pegylated lipids
PolyA	Polyadenylated
PVP	Polyvinylpyrrolidone
RBP	RNA-binding proteins
R_s	Resolution factor
RRD	Regulatory Research Division
ssRNA	Single-stranded ribonucleic acid
TBE	Tris borate EDTA

TEAA	Triethylammonium acetate
UPLC	Ultra performance liquid chromatography
USP	United States Pharmacopeia
UTR	Untranslated regions
UV	Ultraviolet

List of Tables

Table 1. Method parameters for in-house CGE-LIF method and commercial RNA9000 Purity & Integrity kit. 17

Table 2. Summary of quantitative values used to compare the performance of a commercial RNA analysis kit to an in-house CGE-LIF method 21

Table 3.Eight DOE combinations and the associated conditions. 34

Table 4. Peak area (%) composition of mRNA-LNP samples disrupted using different protocols 40

Table 5. Factors and levels in the full factorial design. Three factors chosen to be evaluated at two levels each. 41

Table 6. GLMSELECT Stepwise selection model 45

Table 7. Summary of quantitative values used to compare chromatogram quality 50

Table 8. Peak area (%) composition of mRNA-LNP samples disrupted using different protocols analyzed by IP-RPLC 52

Table 9. Area distribution of mRNA-LNP samples by CGE-LIF after LNP disruption 59

Table 10. Main peak area (%) of FLuc RNA over the course of four weeks stored at different temperatures after extraction from LNPs 60

List of Figure

Figure 1. General structure of *in vitro* transcribed mRNA 2

Figure 2. Structure of cap-0 and cap-1 3

Figure 3. Schematic illustrating polyadenylation.....4

Figure 4. Schematic illustrating mRNA vaccine mechanism of action 5

Figure 5. General overview of *in vitro* mRNA synthesis.....6

Figure 6. Structure of uridine compared to N1-methylpseudouridine 7

Figure 7. Diagram of mRNA encapsulated in a lipid-nanoparticle and lipid components used in COVID-19 vaccines 8

Figure 8. RNA migrating through a gel-filled capillary towards the LIF detector 12

Figure 9. Schematic showing the process of RNA analysis by IP-RP HPLC.....13

Figure 10. Promega RNA markers (red) and kit-provided ssRNA ladder (black) analyzed using the RNA 9000 Purity & Integrity Kit (A) and in-house CGE-LIF method (B) 22

Figure 11. Relationships between migration time and RNA length appear biphasic for both the Promega and kit-provided ladder 24

Figure 12. Different ladders analyzed using the RNA 9000 Purity & Integrity Kit (A) and in-house CGE-LIF method (B) appear to be misaligned.....26

Figure 13. Analysis of Promega RNA markers (red) and NEB ssRNA ladder (blue) by IP-RP HPLC (A) and AGE (B).....28

Figure 14. CGE-LIF traces of Promega RNA markers in various change one factor at a time experiments. 37

Figure 15. Impact of LNP disruption method on CGE-LIF signal intensity 39

Figure 16. Verification of LNP disruption by agarose gel electrophoresis.....40

Figure 17. Two sequences constructed to test 8 combinations of factors in a randomized order 42
Figure 18. CGE-LIF traces of disrupted mRNA-LNP samples over the course of 36 hours in the auto-sampler 42
Figure 19. Electropherograms of each of the 8 combinations of conditions for one set (two sequences) of analyses. 43
Figure 20. Box plots of mRNA main peak percentages for each condition 44
Figure 21. Luciferase RNA spiked with IST analyzed by CGE-LIF (A) and IP-RP HPLC (B) 50
Figure 22. Linear and biphasic relationship between migration time and RNA length by CGE-LIF and IP-RP HPLC 51
Figure 23. mRNA-LNP samples analyzed by CGE-LIF (A) and IP-RP HPLC (B) 52
Figure 24. Comparison of FLuc mRNA-LNP after 5 weeks of storage at 4°C (magenta) to the sample FLuc mRNA-LNP sample after 3 days at 4°C but with the LNP disrupted. 58
Figure 25. FLuc mRNA profile over four weeks stored at -80°C (second row, dark blue), 4°C (third row, magenta), and RT (fourth row, cyan) after extraction from LNPs, with an overall overlay presented in the first row 60

1 Introduction

1.1 mRNA Vaccines and Therapeutics

In recent years, messenger RNA (mRNA)-based therapeutics have emerged as an increasingly promising platform for the treatment and prevention of disease, due to their rapid scalability and their easily modifiable production (*1*, *2*). Unlike traditional protein-based biotherapeutics that deliver target proteins directly, mRNA-based therapies deliver transcripts which are used by host cell machinery to produce functional proteins of interest (*3*, *4*). This approach can be advantageous in its ability to deliver complex or low-yielding proteins, and since mRNA can be rapidly modified to produce different target proteins this platform would enable rapid response to emergencies (*5*). The swift large-scale application and subsequent reformulation of mRNA vaccines during the COVID-19 pandemic demonstrated the safety, efficacy, and ease of production for these products (*6*, *7*). Given this development and the anticipated widespread use of mRNA-based products, reaching a consensus on the critical quality attributes (CQA) of this product class is a strong area of interest.

1.1.1 Structure of mRNA vaccines

mRNA is a single-stranded RNA (ssRNA) copy of DNA that serves as a template for protein synthesis (*1*, *8*). Conventional mRNA-based vaccines encode a target antigen with untranslated regions (UTRs) at either end (5’ and 3’ ends) and take advantage of the host cell machinery to produce a functional protein (*9*). *In vitro* transcribed (IVT) mRNA, like those used in the COVID-19 vaccines, are designed to resemble naturally occurring mRNA in eukaryotic cells; therefore, contain critical elements like the 5’ cap and 3’polyadenylated (polyA) for efficient protein synthesis (Figure 1) (*1*, *10*).

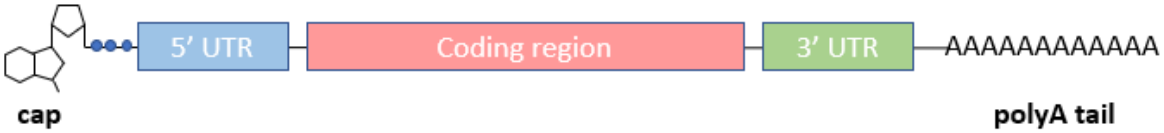

Figure 1. General structure of *in vitro* transcribed mRNA.

1.1.1.1 The 5' cap

5' caps can be enzymatically incorporated through either post-transcriptional or co-transcriptional capping (*11*). In post-transcriptional capping, the 5' cap is added after IVT through a series of enzymatic reactions using the Vaccinia virus capping system. Briefly, the 5'triphosphate end of the nascent RNA is converted to a cap-0 intermediate structure, with a N7-methyl guanosine linked to the 5' nucleotide via a 5'- 5' triphosphate linkage (Figure 2) (*12–14*). The cap-0 intermediate is further methylated at the 2'hydroxyl group of the first nucleotide proximal to the cap to produce a cap-1 structure. In eukaryotes, this enzymatic process occurs co-transcriptionally as soon as the first 25-30 nucleotides (nt) are transcribed (*12*, *13*). The mRNA 5' cap is crucial for many functions, including the regulation of nuclear splicing, and the facilitation of nuclear transport and translation (*15*). Furthermore, the cap-1 structure is recognized by the immune system as a marker of self mRNA which protects it from degradation by immunomodulatory proteins (*15-18*).

In co-transcriptional capping, a cap analog is added to the IVT reaction to produce a 5' capped mRNA. The cap is directly incorporated at the 5' end and cannot be added within a growing transcript because it lacks a free 5'-triphosphate (*18*).

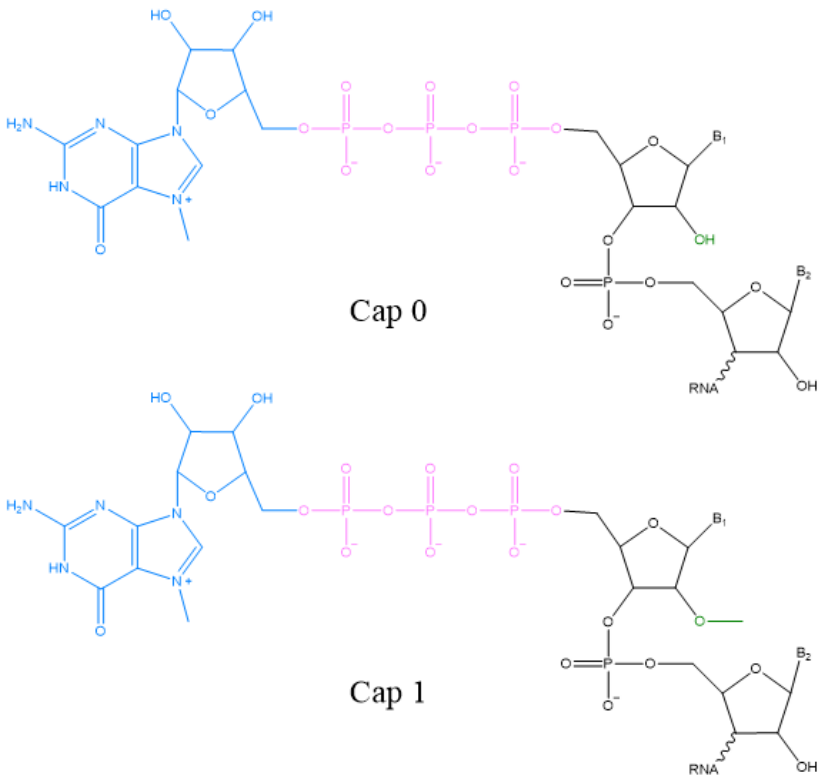

Figure 2. Structure of cap-0 and cap-1.

1.1.1.2 The UTRs and 3' polyA tail

UTRs are non-coding regulatory elements that help regulate mRNA stability and promote translation efficiency through interactions with RNA-binding proteins (RBP) (*5*). Like the mRNA coding region, UTRs can be designed and optimized to modulate the rate of mRNA degradation and increase the rate of protein translation. The polyA tail, an extension of the 3' UTR, is a chain of 100 – 250 adenosines that protects the mRNA 3' terminal from degradation (Figure 3) (*15*, *20*). As with the 5' cap, the polyA tail can be incorporated co-transcriptionally from a DNA template, or post-transcriptionally through a series of enzymatic reactions (*19*).

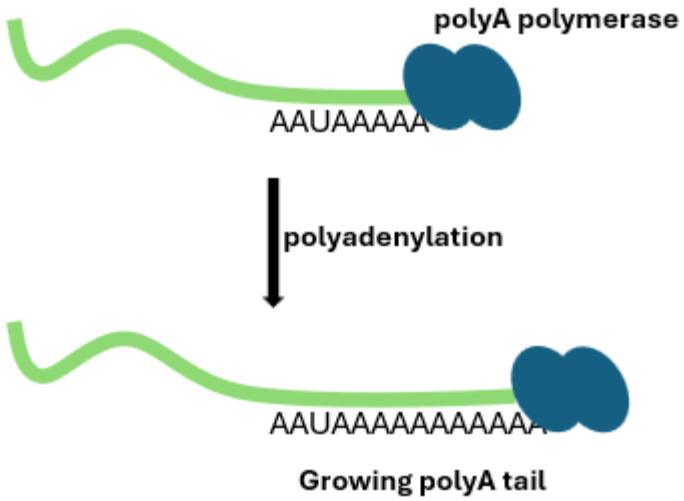

Figure 3. Schematic illustrating polyadenylation. A polyA tail is added to the 3' end of an RNA transcript by a polyA polymerase.

1.1.2 Mechanism of action

mRNA vaccines and therapies deliver mRNA encoding a specific protein or antigen to the host cell where it is translated into proteins using the host machinery (*3*, *20*). Once the proteins are translated they are presented on the cell surface as antigens and elicit an immune response (Figure 4) (*22*, *23*).

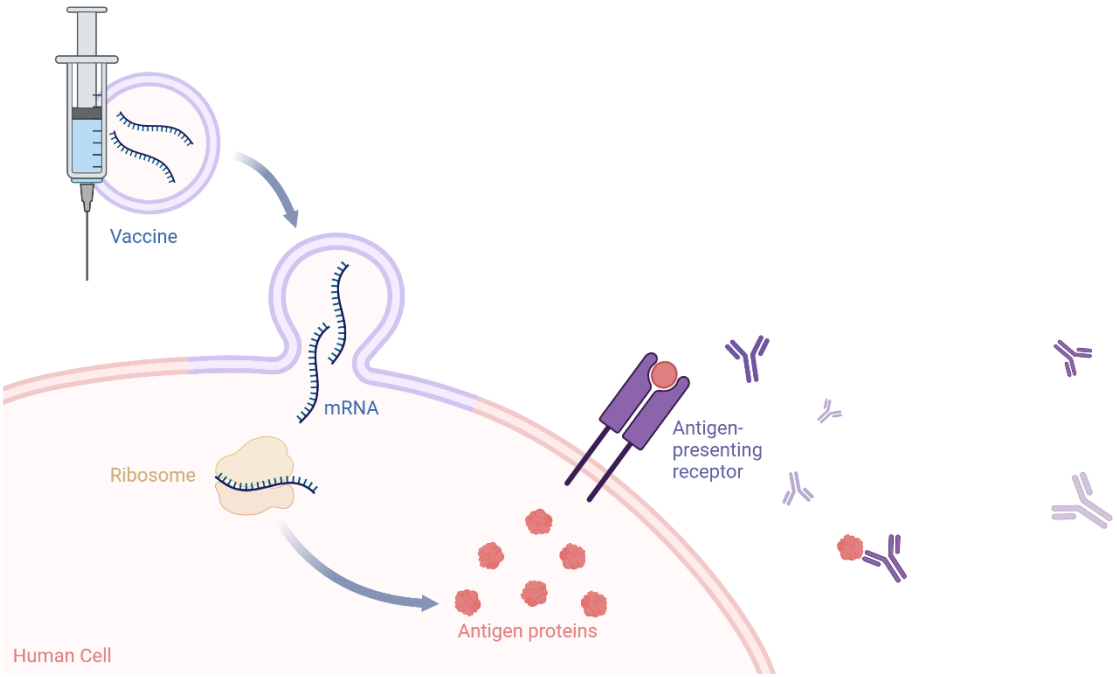

Figure 4. Schematic illustrating mRNA vaccine mechanism of action. mRNA encoding a target antigen is delivered to the host cell in a lipid-nanoparticle. The mRNA is released into the cytoplasm where the host translation machinery is used to produce the antigen proteins. The protein is presented on the cell surface as an antigen where it interacts with antibodies of immune cells to elicit an immune response. Created with Biorender.com

1.1.3 General manufacturing process

The process of mRNA-LNP vaccine production (Figure 5) starts with a DNA template encoding the antigen of interest and an upstream T7 RNA polymerase promoter. While many modified nucleosides are possible, the two currently approved mRNA vaccines substitute uridine with 1-methylpseudouridine (Figure 6), a synthetic pyrimidine, to reduce the immunogenicity of the mRNA (*5*, *23*–*25*). Capping and tailing can occur during or after the IVT reaction as described in chapter 1.1.1. Some manufacturers opt for co-transcriptional capping using the TriLink CleanCap® technology while others incorporate the cap in a separate post-transcriptional reaction (*24*). DNase I and Proteinase K are added in a post-reaction cleanup to remove the DNA template and inactivate any nucleases that might

degrade the mRNA. Before any further processing, the mRNA is concentrated and purified by flow filtration to remove potential impurities (*26*, *27*). At the end of these steps a concentrated mRNA drug substance (DS) is obtained. To get to the final drug product (DP), the DS must undergo release testing and finally aseptic filling and finishing (*28*).

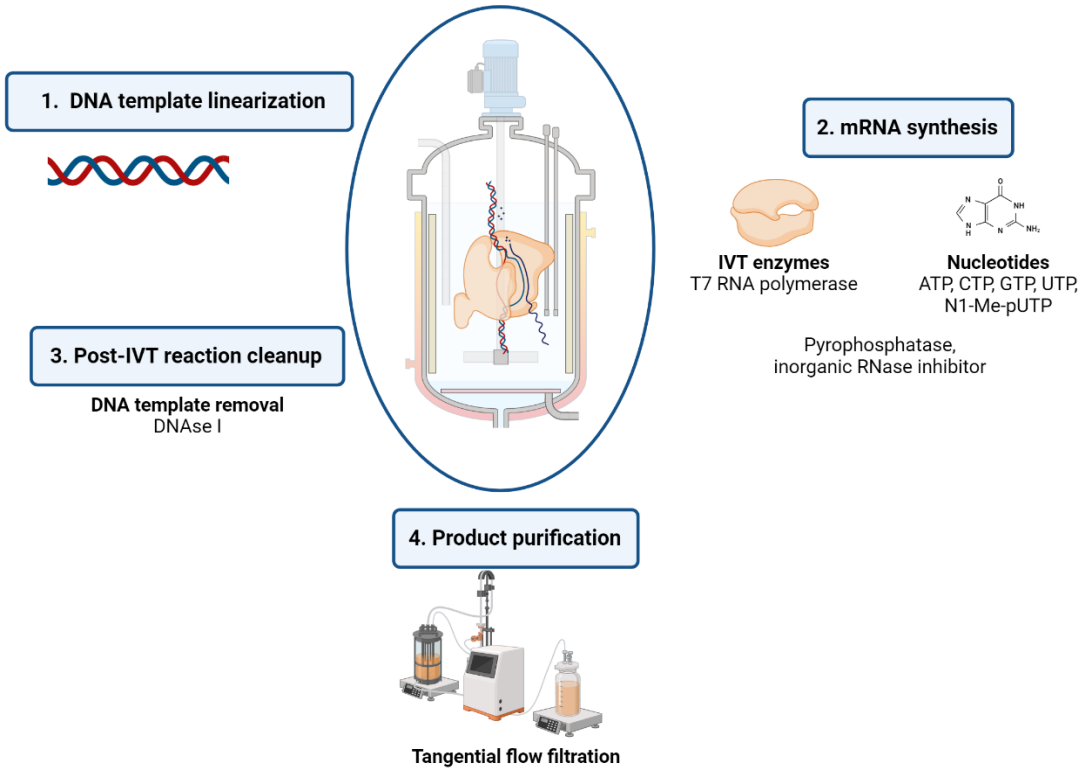

Figure 5. General overview of *in vitro* mRNA synthesis. Created with Biorender.com

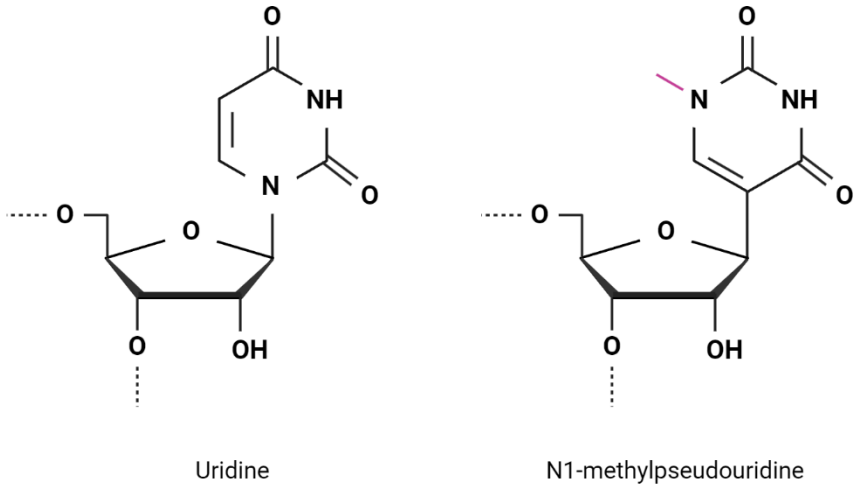

Figure 6. Structure of uridine compared to N1-methylpseudouridine. N1-methyluridine is able to form a canonical base pair with adenine as uridine would. However, the additional methyl group (purple) causes steric hindrance and prevents Toll-like receptor 7 (TLR7) binding and subsequent immune activation.

1.1.4 Lipid nanoparticles delivery system

Initially, the inherent instability of mRNA and the lack of an efficient *in vivo* delivery system were major bottlenecks in the development and subsequent application of mRNA-based vaccines (*8*, *21*, *29*). mRNA molecules are highly susceptible to degradation via RNases, which are ubiquitous environmental contaminants, necessitating a suitable carrier for *in vivo* administration (*29*). This challenge was largely overcome through the use lipid nanoparticles (LNP) (*30–32*). LNP used in COVID-19 vaccines are composed of four lipids: cationic ionizable lipid that interacts with the negative mRNA backbone, pegylated (PEG) lipids, phospholipids, and cholesterol that contribute to the structure and stability of the LNP (Figure 7). The LNP encapsulates mRNAs in its hollow core, protecting mRNAs from degradation while facilitating cellular uptake.

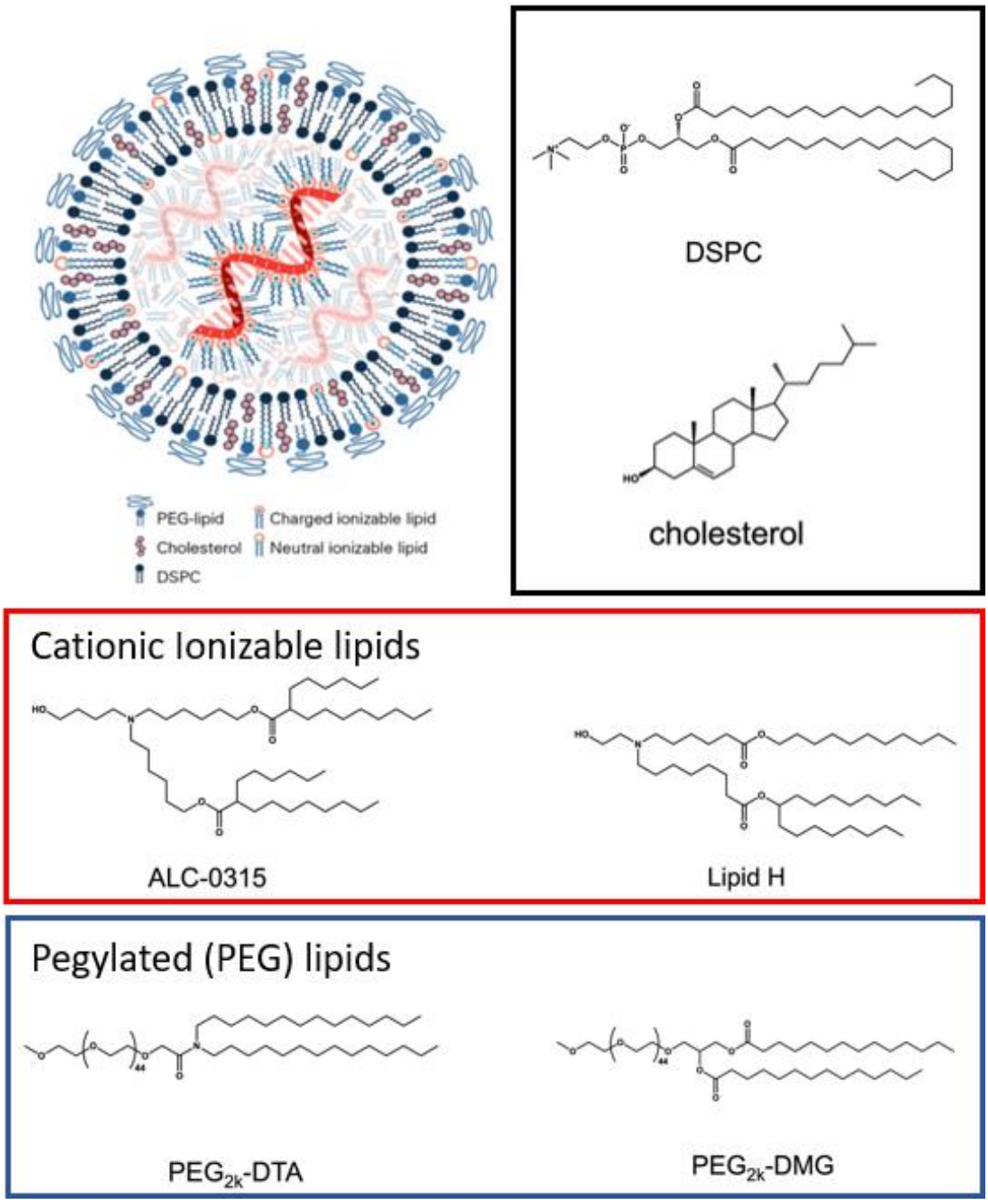

Figure 7. Diagram of mRNA encapsulated in a lipid-nanoparticle and lipid components used in COVID-19 vaccines.

1.1.4.1 LNP encapsulation and mechanism of delivery

mRNA-LNP assembly is a complex physical process involving the assembly of many components (*32*, *33*). When the LNP components are mixed with mRNA in an aqueous

buffer at approximately pH 4 the ionizable lipid component is protonated and interacts with the anionic phosphate backbone of mRNA *via* electrostatic interactions. The hydrophobic effect then drives lipid vesicle formation around the mRNA – encapsulating it. Following vesicle formation, the pH is adjusted to physiological pH (7.4) neutralizing the previously cationic ionizable lipids. This further increases hydrophobicity and drives the vesicles to fuse, completely sequestering the ionizable lipids and mRNAs in the centre (Figure 7). Upon vaccine administration, mRNA-LNPs are endocytosed by the host cell. The acidic pH (4.5-6.5) of the endosome drives protonation of the ionizable lipids. Once this occurs, the cationic lipids will effectively flip outward to facilitate endosomal release of mRNA into the cytoplasm where it is translated into protein (Figure 4) (*32–34*).

1.2 Current Regulatory Guidelines and the Need for Standardization

The assessment of mRNA-LNP products is crucial to ensure their quality and potency. Currently, there are no comprehensive guidelines regarding the assessment of these products making their evaluation and regulation challenging. Pharmacopeial organizations like the United States Pharmacopeial (USP) Convention and the European Medicines Agency (EMA) are working to establish standards and regulatory references for mRNA vaccines (*35–37*). However, the novelty of the platform presents considerable challenges. While the physical properties of RNA are well-defined in a laboratory context, their attributes in a biotherapeutic context are not as well explored, especially in comparison to protein-based therapeutics, which have an extensive history of development (*2*, *38*, *39*). This makes it difficult for the USP and EMA to set acceptable limits for impurities and critical quality attributes, which are crucial for ensuring product quality.

Standardized practices and analytical methods for the assessment of mRNA-LNP products are essential. Standardization through pharmacopeial monographs not only ensures consistency among different manufacturers but also promotes a shared understanding of mRNA products across regulatory bodies and international authorities. The demand for robust and well-understood analytical methods with accurate and reliable detection is critical for quality control, especially considering the pivotal role of mRNA vaccines in tackling global health challenges (*40*, *41*).

1.2.1 mRNA vaccine impurities and critical quality attributes

The process of IVT can leave behind many impurities such as: residual DNA template, free nucleotides, dsRNA, truncated RNA and other process related impurities (*42*). Though many of these impurities can be removed through post-IVT cleanup reactions (DNase I treatment) and filtrations prior to product release, analytical methods are necessary to ensure their removal. Furthermore, other manufacturing impurities may still arise downstream, such as the RNA-lipid adducts observed by the Packer group (*43*). Such impurities may have biological impacts; therefore, it is imperative that they are identified and appropriately assessed (*37*).

CQA are key parameters or characteristics of a pharmaceutical product that must be controlled within defined limits to ensure consistent quality, efficacy, and safety. They are typically identified during development and manufacturing based on the understanding of the product and are often linked to desired clinical outcomes (*37*). For mRNA-based therapeutics, transcript length or mRNA integrity is of particular importance as it is often used as a stability-indicating attribute. As such, one clear critical quality attribute is transcript length. Several unique properties of mRNA and its manufacturing process necessitate the

assessment of transcript fragmentation for monitoring product stability (*44*). As mentioned previously, critical elements at the 5' and 3' termini of mRNA are required for efficient protein synthesis and these will only be preserved in the full-length molecule (*45*). Furthermore, the process of mRNA synthesis relies on enzymes, which tend to produce a mixture of products with different lengths that are difficult to separate and identify (*46*). Finally, mRNA molecules are inherently susceptible to cleavage by hydrolysis in aqueous conditions and RNases, compromising their stability after manufacturing. Although encapsulation in LNP offer significant protection against these processes, mRNA fragmentation remains a concern for long-term stability (*47*). Thus, the length profile of a transcript is a stability indicating CQA likely to fluctuate between batches, products, and over time. As the degradation of mRNA is difficult to control and eliminate, it is crucial to understand how impurities can form and develop standardized analytical methods to detect them. This approach not only safeguards product quality but also enhances reliability in clinical outcomes, underscoring the importance of robust quality assurance in mRNA biotherapeutic development.

1.3 Analytical Methods Used for the Assessment of mRNA Integrity

Following the first mRNA vaccines, an initial consensus of analytical methods was formed from both research and manufacturing experience (*22, 35, 48*). Amongst them, capillary gel electrophoresis (CGE) and ion-pair reversed-phase liquid chromatography (IP-RPLC) were the bioanalytical techniques of choice for assessing transcript length and the percentage of fragments (*49, 50*).

1.3.1 Capillary gel electrophoresis

In CGE, nucleic acid analytes are usually electrokinetically injected and migrate through a capillary containing a gel sieving matrix, typically with denaturing additives (Figure 8). These analytes are separated by size as larger fragments migrate slower through the matrix (*51*). Although commonly for used for DNA oligonucleotide analysis, several groups have explored various CGE parameters, and additives to improve analysis for large mRNA molecules, mostly in a research context (*52–55*). In the biotherapeutic context, CGE-LIF is commonly proposed for measuring RNA integrity or "intactness" (*35*, *49*).

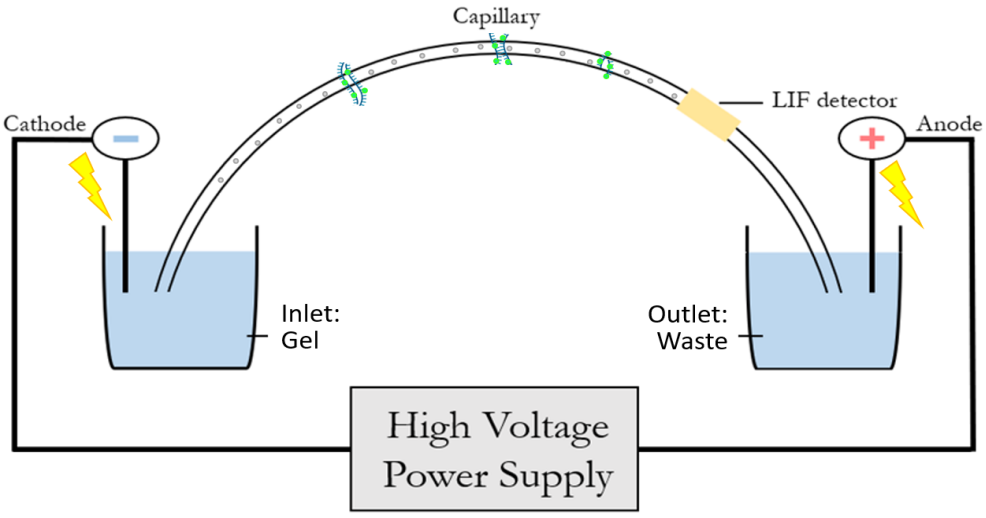

Figure 8. RNA migrating through a gel-filled capillary towards the LIF detector.

1.3.2 Ion-pair reversed-phase liquid chromatography

IP-RPLC is a chromatographic technique widely used to analyze DNA. In recent years its application has been extended to RNA analysis (*56*). This technique uses alkylammonium salts to complex the mRNA phosphate backbone, increasing its affinity for the non-polar stationary phase (Figure 9) (*57*). RNA is eluted using a mobile phase containing an organic

solvent; longer nucleic acids have increased affinity to the column, requiring a higher organic content in the mobile phase for elution. Similar to CGE, IP-RPLC is commonly used for oligonucleotide analysis (*57*, *58*) and increasingly explored for longer analytes (*43*, *59*, *60*).

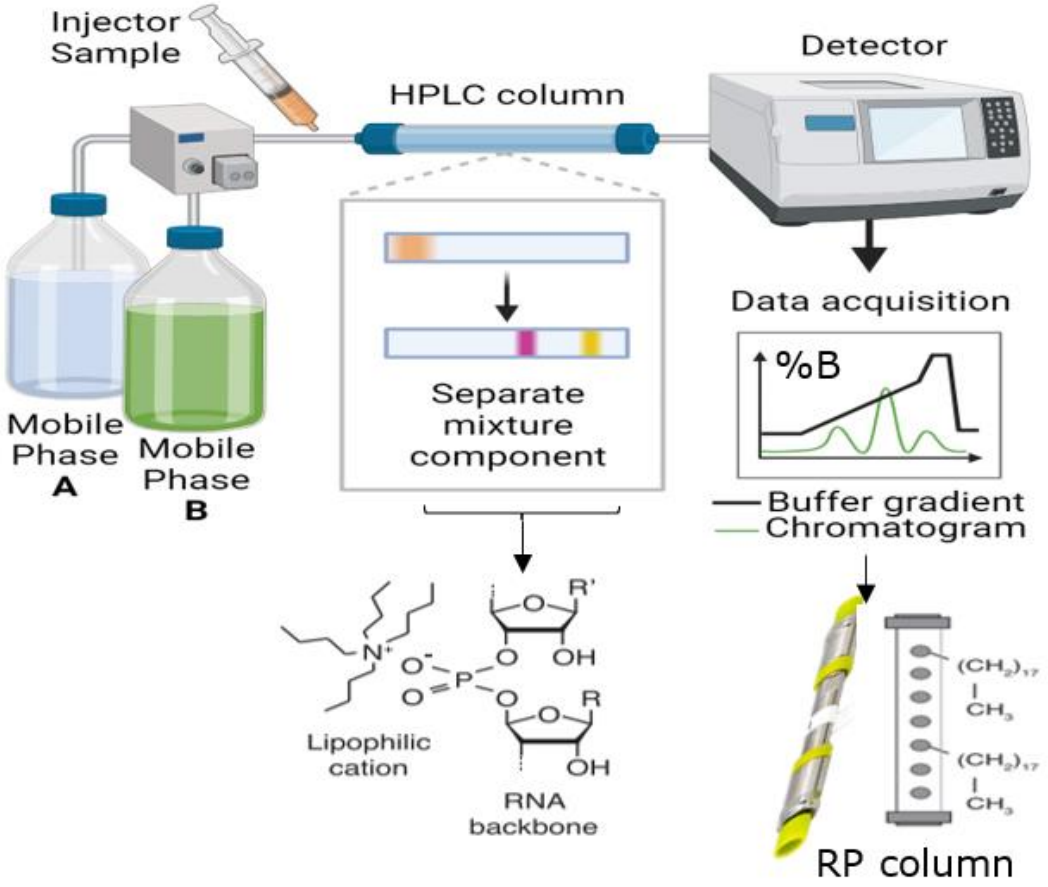

Figure 9. Schematic showing the process of RNA analysis by IP-RP HPLC.

1.4 Research Objectives

Since mRNA are precursors to the therapeutic protein there is substantial reliance on physicochemical aspects such as mRNA integrity as predictors of product effectiveness. As such we depend heavily on physicochemical assays like CGE and IP-RPLC to assess

integrity. While CGE and IP-RPLC are orthogonal methods for mRNA length analyses, CGE commonly achieves higher sensitivity and resolution for lower sample volumes, particularly when paired with a laser-induced fluorescence (LIF) detector (*42*, *61*, *62*). However, sample injectors and detectors in modern liquid chromatography systems provide significantly improved assay-to-assay variability, making chromatography an effective method for quantifying product content and related impurities in a routine environment. There are many research gaps especially in the biotherapeutic context (*43*, *49*). Therapeutic products do not only contain mRNA – formulated products include lipids and other excipients that have the potential to interfere with analytical assays (*63*). As current mRNA therapeutics are formulated with LNPs there is potential to form mRNA-lipid adducts. Indeed, such impurities have been previously reported by Packer *et al*., (*43*) to negatively impact product efficacy. Furthermore, they report that these lipid-adducts were detectable by IP-RPLC but not by capillary electrophoresis. While both CGE and IP-RPLC are powerful physicochemical techniques for assaying mRNA length, they operate on different mechanisms of separation which has the potential to bias the detected impurity profile. Given these differences and the impacts of impurities and fragmentation to the efficacy of mRNA biotherapeutics, it is important to assess the suitability of the techniques and standardize their applications.

Although a foundation of understanding is gradually forming in the biotherapeutic context of mRNA (*43*, *49*, *64–69*), analyzing and standardizing mRNA quality attributes remain challenging. Most studies have examined in vitro transcribed mRNA free in solution. However, some studies have shown that lipid nanoparticle encapsulation is important in assessing the product purity profile (*43, 60, 66*). Thus, understanding the advantages and

limitations of each technique, particularly the detection capabilities and associated impurity profiles are crucial. This understanding is especially important in the context of biotherapeutics, where mRNA is modified and encapsulated, and will be critical for making accurate mRNA product comparisons and designing practical reference standards.

The project aims to achieve two primary objectives: (1) fill the knowledge gap regarding mRNA assessment in the context of biotherapeutics, and (2) contribute to standardization efforts by providing insight into the performance of two different analytical methods used for mRNA integrity assessment. This involves addressing the challenges associated with comparing results and facilitating more effective product-to-product assessments in the expanding landscape of mRNA applications.

2 Comparative analysis of commercial and in-house capillary gel electrophoresis for RNA separation

2.1 Background

Capillary gel electrophoresis has emerged as a pivotal tool in the separation of mRNA, offering high-resolution separation capabilities essential for analyzing mRNA integrity (*42*, *49*, *51*, *52*). While various specialized instruments and kits have been marketed for capillary electrophoresis analysis of mRNA drug products (*70*), their proprietary nature can limit method customization and research. In contrast, the development of in-house CGE methods presents a compelling alternative, offering several advantages.

One major advantage of in-house CGE methods is the ability to tailor them specifically to research needs. Buffer compositions, separation matrices, and running conditions can be optimized to achieve ideal resolutions and sensitivity depending on RNA fragment lengths. This flexibility allows for adjustments to experimental protocols as new insights or requirements emerge. Additionally, in-house CGE methods can be more cost-effective, eliminating the need for expensive proprietary reagents and consumables associated with commercial kits.

The objective of this chapter was to compare the performance of an in-house CGE-LIF method developed based on a Technical Note (*71*) to an existing commercial RNA analysis kit. Both the Technical Note and commercial kit were developed by the same company; method parameters for both methods are outlined in Table 1. This section aims to provide a comprehensive overview of the strengths and limitations of the two approaches. The analyses will inform researchers on practical considerations and potential trade-offs involved in

selecting an appropriate CGE method for their specific applications, ultimately contributing to more informed decision-making in laboratory practices.

Table 1. Method parameters for in-house CGE-LIF method and commercial RNA9000 Purity & Integrity kit.

Parameter	In-house CGE method	Commercial Kit
Gel buffer composition	1% PVP + 4 M urea + 1X TBE	Unknown
Dye	0.02% (v/v) SYBR Green II	0.02% (v/v) SYBR Green II
Injection voltage	5.0 kV	1.0 kV
Injection time	5 s	3 s
Separation voltage	6.0 kV	6.0 kV

2.2 Materials and Methods

2.2.1 Reagents and samples

RNA 9000 Purity & Integrity Kit (C48231) was purchased from AB Sciex (Massachusetts, USA). RNA markers (281 – 6583 b; G3191) was purchased from Promega Corporation (Wisconsin, USA). ssRNA ladder (0.5 – 9 kb; N0362) and Nuclease-free Water (NFW; B1500L) were purchased from New England Biolabs (Massachusetts, USA). Diethyl pyrocarbonate (DEPC)-treated water (AM9916), LC-MS grade water (W6-4), acetonitrile (A955-4), Tris-Borate-EDTA (TBE) buffer (B52), SeaKem™ ME Agarose (BMA50010), formamide (17899), and SYBR™ Green II (S7564) were purchased from Thermo Fisher Scientific (Massachusetts, USA). Urea (U1250), polyvinylpyrrolidone (PVP; 437190), and dibutylammonium acetate (DBAA; 625718) were purchased from MilliporeSigma (Missouri, USA). Triethylammonium acetate (TEAA; A5702) was purchased from TCI America (Oregon, USA).

2.2.2 Sample preparation for CGE-LIF analysis

Commercial RNA ladders were analyzed to compare the performance of the two CGE methods. The Promega RNA markers was diluted to 0.025 mg/mL in nuclease free water and the ssRNA ladder was diluted 25-fold in NFW. Both were heat denatured at 70°C for 2 minutes then chilled on ice before being loaded into the instrument.

2.2.3 Instrumentation

CGE analyses were performed on a PA800 Plus Pharmaceutical Analysis System (AB Sciex) equipped with a solid-state laser-induced fluorescence detector (λex = 488 nm/λem = 520 nm) using a 30 cm bare fused silica capillary (effective length: 20 cm, internal diameter: 50 μm). Prior to its first use, the capillary was conditioned with a series of rinses as follows: 0.1 M NaOH, DEPC-treated water, 0.1 M HCl, and DEPC-treated water, each injected at 20 psi for 5 minutes.

IP-RPLC analyses were performed on a Waters Alliance e2695 Separation Module (Waters) equipped with PDA detector and fluorescence detector models. Sample separation was performed using a DNAPac RP column with 4 μm particles (length: 100 mm and internal diameter: 2.1 mm).

2.2.4 Commercial CGE-LIF RNA analysis kit

Commercial RNA 9000 Purity & Integrity Kit was used to analyze RNA ladders per vendor instructions (*72*). Briefly, 10 μL of the provided SYBR™ Green II RNA Gel Stain (500X) was added to 5 mL of Nucleic Acid Extended Range Gel. The kit-provided ladder was diluted 25-fold in NFW and denatured at 70°C for 2 minutes then chilled on ice before being loaded into the instrument. Separation was performed on the instrument and capillary as

indicated in chapter 2.2.3. Samples were maintained at 10°C in the autosampler until electrokinetic injection using reversed polarity mode (anode on detection side) at 1 kV for 3 seconds. Separation was achieved by applying a voltage across the electrodes at 6 kV for 22 minutes while the cartridge temperature was maintained at 30°C. Data acquisition was performed using the 32Karat (version 10.1) software (AB Sciex), and analysis was performed using the Empower 3 (version 7.21) software (Waters).

2.2.5 In-house CGE-LIF method parameters and analysis

For each separation the capillary was filled with gel buffer (1% PVP, 4M urea, 1X TBE and 0.02% (v/v) SYBR^{TM} Green II (10,000X); pH = 8.6; prepared day-of) by applying 50 psi for 5 minutes. Samples were maintained at 4°C in the autosampler until electrokinetic injection using reversed polarity mode (anode on detection side) at 5 kV for 5 seconds. Separation was achieved by applying a voltage across the electrodes at 6 kV for 20 minutes while the cartridge temperature was maintained at 25°C. Data acquisition was performed using the 32Karat (version 10.1) software (AB Sciex), and analysis was performed using the Empower 3 (version 7.21) software (Waters).

2.2.6 Agarose gel electrophoresis

Agarose gel electrophoresis (AGE) was performed to compare the migration of the different RNA ladders. A 1% (w/v) agarose solution in 1X TBE buffer was boiled before 0.001% (v/v) SYBR Green II was added. The gel mixture was poured into the gel cassette and covered with aluminum foil then left to airdry. Samples were loaded on the gel at equal concentrations; electrophoresis was performed in 0.5X TBE buffer run at 180 V for 30 minutes. After the run, the gel was visualized using a ChemiDoc XRS+ System (Bio-Rad).

2.2.7 IP-RP HPLC

IP-RP-HPLC was additionally performed to determine if separation mechanisms had an impact on the migration of the different RNA ladders relative to each other. A method from Packer *et al.,* (*43*) was adapted to operate on available instrumentation. Flow rate was maintained at 0.35 mL/min and a column temperature of 60°C was used. Mobile phase A consisted of 50 mM DBAA, and 100 mM TEAA and mobile phase B consisted of 50% acetonitrile, 50 mM DBAA, and 100 mM TEAA. 10 µL of sample (0.1 mg/mL) was injected for each analysis, and mRNA was detected by UV at 260 nm. Data acquisition and analysis were performed using the Empower 3 (version 7.21) software (Waters).

2.3 Results and Discussion

Method comparison was conducted by analyzing the Promega RNA markers containing nine fragments (0.28 kb – 6.2 kb), as well as the kit-provided ssRNA ladder containing ten fragments (0.05 kb – 9 kb) using both the commercial kit and the in-house method. Method performance was scored based on the ladder linearity, and resolution factors between fragments.

2.3.1 Head-to-head comparison of commercial kit and in-house CGE method for separation of RNA ladders

The initial comparison of RNA ladder separation by the two CGE methods revealed a clear difference in resolution and fragment visibility (Figure 10). The resolution factors (Rs; calculation shown in Appendix 9.2) at the low and high molecular weight (MW) ranges revealed that the commercial kit (Figure 10A) offers higher resolution than the in-house method (Figure 10B) for both the kit-provided ssRNA ladder and the Promega RNA markers (Table 2). The resolution difference was especially apparent at the higher MW (>2 kb) for

the Promega RNA markers, where baseline resolution was achieved using the commercial kit but not the in-house method. When the kit-provided ssRNA ladder was analyzed using the in-house CGE method, only nine of the ten fragments are visible. The last two fragments (7 kb and 9 kb) appear to comigrate forming a broader peak indicating that the in-house CGE method is not suitable for resolving RNA fragments at this particular size range. This is further evident when the linearity of the ladders was examined for each of the methods (Table 2).

Table 2. Summary of quantitative values used to compare the performance of a commercial RNA analysis kit to an in-house CGE-LIF method. Values were calculated based on the average of duplicates (n = 2) for each combination of ladders and separation methods.

Method	Ladder	Linearity of RNA ladder (R2)			Resolution Factor (Rs)	
		Full Range	Low MW (<2 kb) range	High MW (>2 kb) range	Low MW*	High MW**
In-house CGE	Promega	0.988	0.994	0.958	3.43	2.03
	Kit-provided	N/A***	0.993	N/A***	1.40	1.56
Commercial Kit	Promega	0.963	0.996	0.995	5.53	2.24
	Kit-provided	0.976	0.960	0.986	2.73	1.70

*Rs was calculated using the values of the 0.623 kb and 0.981 kb peaks for the Promega RNA markers and using the values of the 0.5 kb and 1 kb peaks for the kit-provided ladder.
**Rs was calculated using the values of the 3.683 kb and 4.981 kb peaks for the Promega RNA markers and using the values of the 5 kb and 7 kb peaks for the kit-provided ladder.
**9 kb peak omitted.

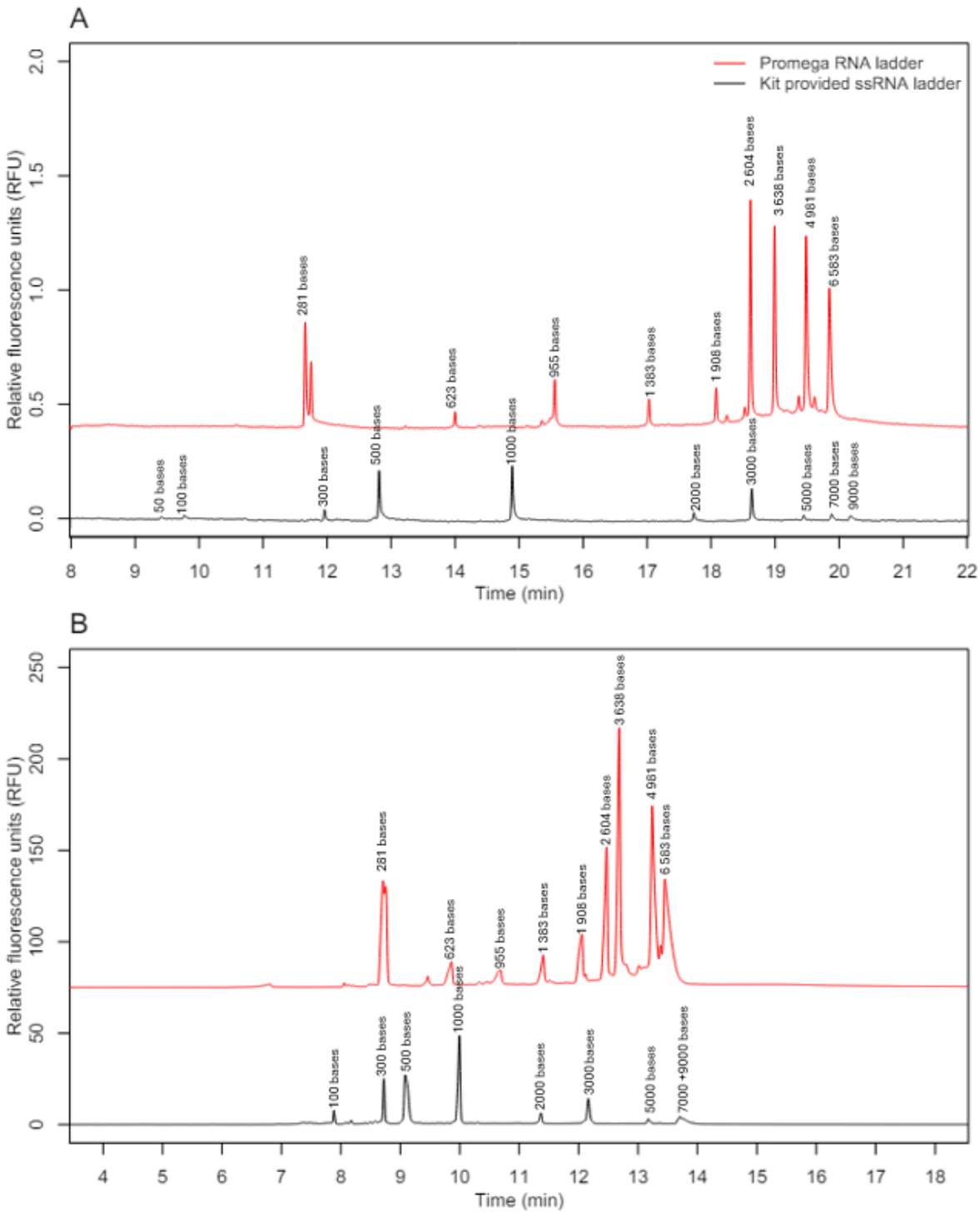

Figure 10. Promega RNA markers (red) and kit-provided ssRNA ladder (black) analyzed using the RNA 9000 Purity & Integrity Kit (A) and in-house CGE-LIF method (B). Both ladders are clearly resolved when analyzed with the commercial kit, but not with the in-house method. The two largest fragments (7 kb and 9 kb) of the kit-provided ladder are not resolved and appear to comigrate when the in-house CGE method was used.

Fragments between the ladders are misaligned from the 1 kb to 5kb range. CGE-LIF analyses were performed in duplicates (n = 2).

Linearity is often used to determine the suitability of a method for a given fragment size range. When linearity was calculated across the entire range of the ladders, the commercial kit exhibited slightly higher linearity for the kit-provided ladder ($R^2 = 0.976$) than the Promega RNA markers ($R^2 = 0.969$). Interestingly, a different observation was made using the in-house method. While the linearity of the kit-provided ladder could not be accurately calculated, due to the poorly resolved 7 kb and 9 kb peaks, the linearity of the Promega RNA markers ($R^2 = 0.988$) was higher than that of the commercial kit. This indicated that the in-house gel is more suitable for the separation of fragments of this particular size range (0.2 – 6.5 kb) but not for the separation of RNA above the 7 kb in length. When the relationship between migration time and RNA length was plotted for each combination of ladder and method, we noticed that the linear regression demonstrated a biphasic fit Figure 11).This prompted us to consider the RNA fragments in each ladder as two separate regimes (low and high MW). When the linearities were recalculated with this in mind, we observed that the relationship between migration time and RNA length exhibits high linearity from 0.1 kb up to 2 kb for both methods. Beyond this point the linearity by the in-house method noticeably decreases compared to the commercial kit. This observation is consistent with a study by Todorov *et al*., where they demonstrate that RNA mobility and migration through a matrix is dependent on its viscosity (*73*). In the study, Todorov *et al.*, explains that every semi dilute polymer matrix has a concentration or ‘entanglement threshold’ above which the polymer molecules form a flexible network. Above this entanglement threshold, two mobility regimes for RNA are observed – similar to what is shown in Figure 11. The study suggests that for each semi dilute polymer system and entanglement threshold there is a corresponding critical

length of RNA, beyond which point separation efficiency is diminished. This suggests that a single gel buffer composition is not ideal for the separation and analysis of a large range of RNA sizes.

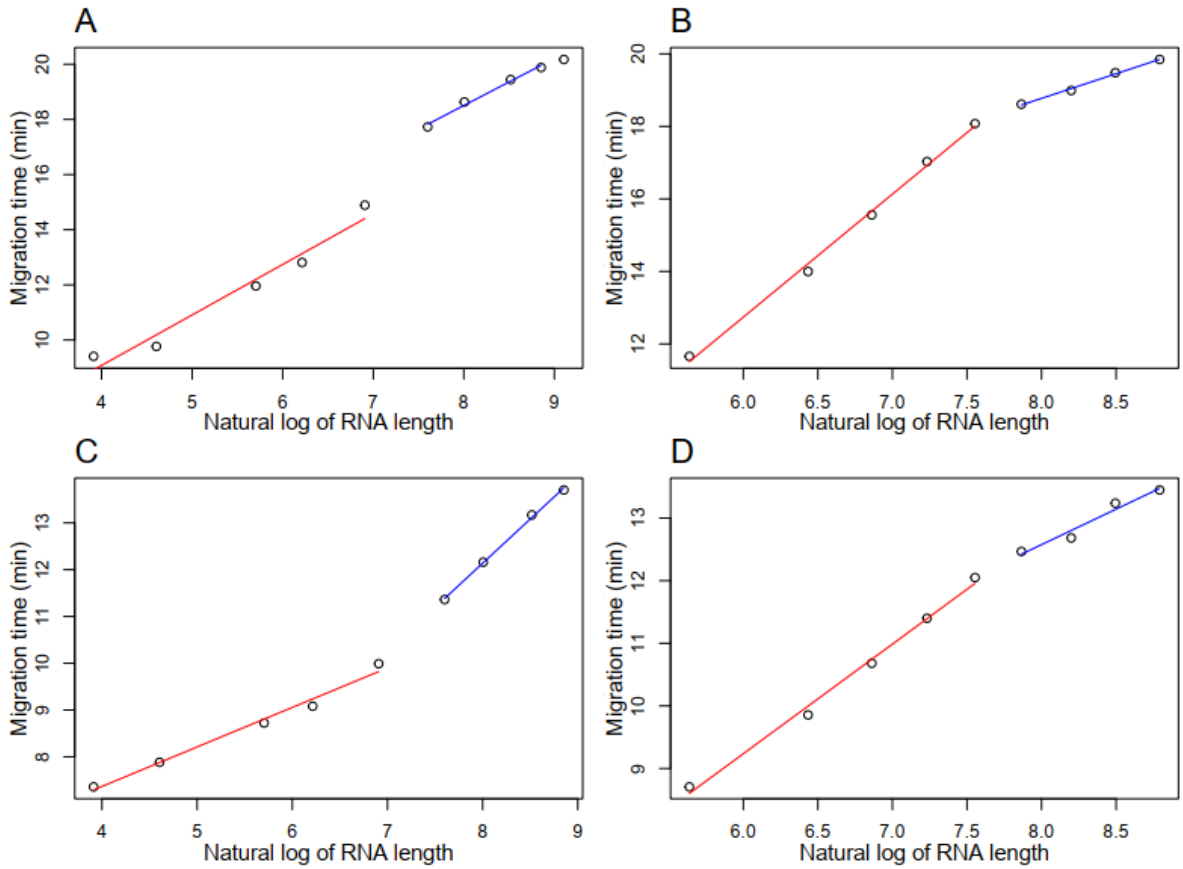

Figure 11. Relationships between migration time and RNA length appear biphasic for both the Promega and kit-provided ladder. The linearity of the kit-provided ladder by the commercial kit (A) and in-house method (C), and the Promega ladder by the commercial kit (B) and in-house method (D) exhibit biphasic linearity with a breakpoint of approximately 2 kb. Linear regressions were fitted on the natural logarithmic plots of RNA size as a function of migration time. The red line is fitted to fragments with lengths up to 2 kb, and the blue to fragments above 2 kb. CGE-LIF analyses were performed in duplicate (n = 2) for all combinations of ladders and separation methods.

To further test the method performance and robustness another RNA ladder from a different vendor (NEB) was analyzed using both methods (Figure 12). Coincidentally, the NEB ssRNA ladder trace overlays exactly with the kit-provided ladder with the exception of the

three smallest fragments (0.05, 0.1, and 0.3 kb) that were not present in the NEB ladder. As expected, the observations made with the kit-provided ladder were applicable to the NEB ladder: the NEB ssRNA ladder was well-separated and all fragments were visible when separated using the commercial kit. When analyzed with the in-house method the same larger peak was observed at the end, a result of the 7 kb and 9 kb fragments comigrating. Fragment comigration is a resolution deficit that could potentially lead to inaccuracies in size determination RNA molecules in that range.

We also observed that first peak of the Promega ladder consistently splits into a doublet when analyzed with the commercial kit. Because of its proprietary nature and lack of transparency regarding buffer composition we were unable to determine the cause of this anomaly.

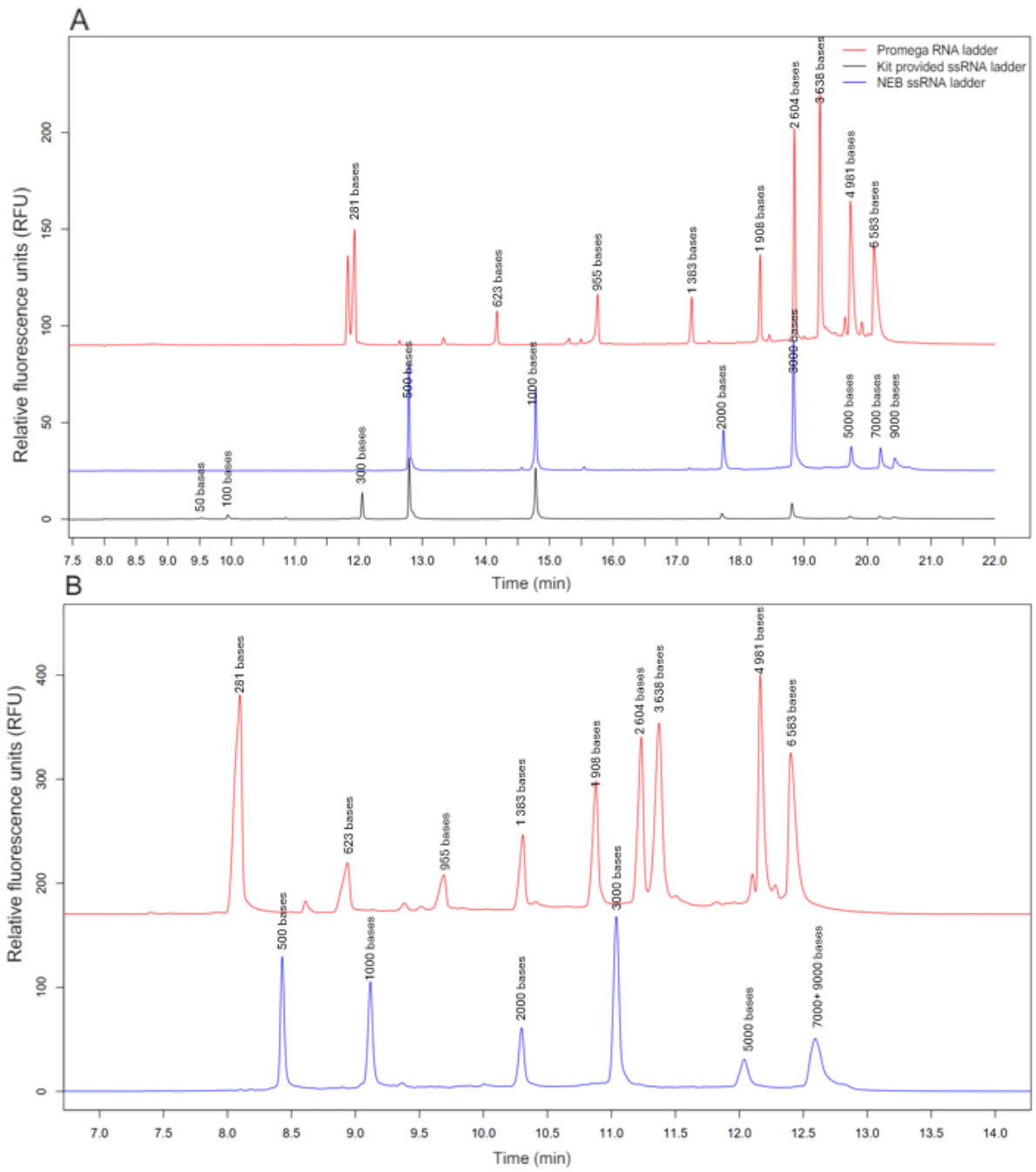

Figure 12. Different ladders analyzed using the RNA 9000 Purity & Integrity Kit (A) and in-house CGE-LIF method (B) appear to be misaligned. The kit-provided ssRNA ladder (black) and the NEB ladder (blue) align exactly from 0.5 kb to 9 kb. Fragments between the Promega RNA markers (red) and the others are misaligned from the 1 kb to 5kb range. CGE-LIF analyses were performed in duplicate (n = 2).

2.3.2 Investigation of RNA ladder misalignment

The use of RNA ladders is a common practice to determine size and integrity of RNA molecules during separation and analysis. However, discrepancies can arise when different RNA ladders appear to misalign as previously observed when the various RNA ladders were analyzed by CGE-LIF (Figure 12). In this case, the 2 kb fragment of the kit-provided ladder appeared to align with the 1.3 kb fragment of the Promega RNA markers. To determine if the source of the misalignment was related to the mechanism of separation or product-related, the ladders were analyzed by orthogonal methods, AGE, and IP-RP HPLC (Figure 13).

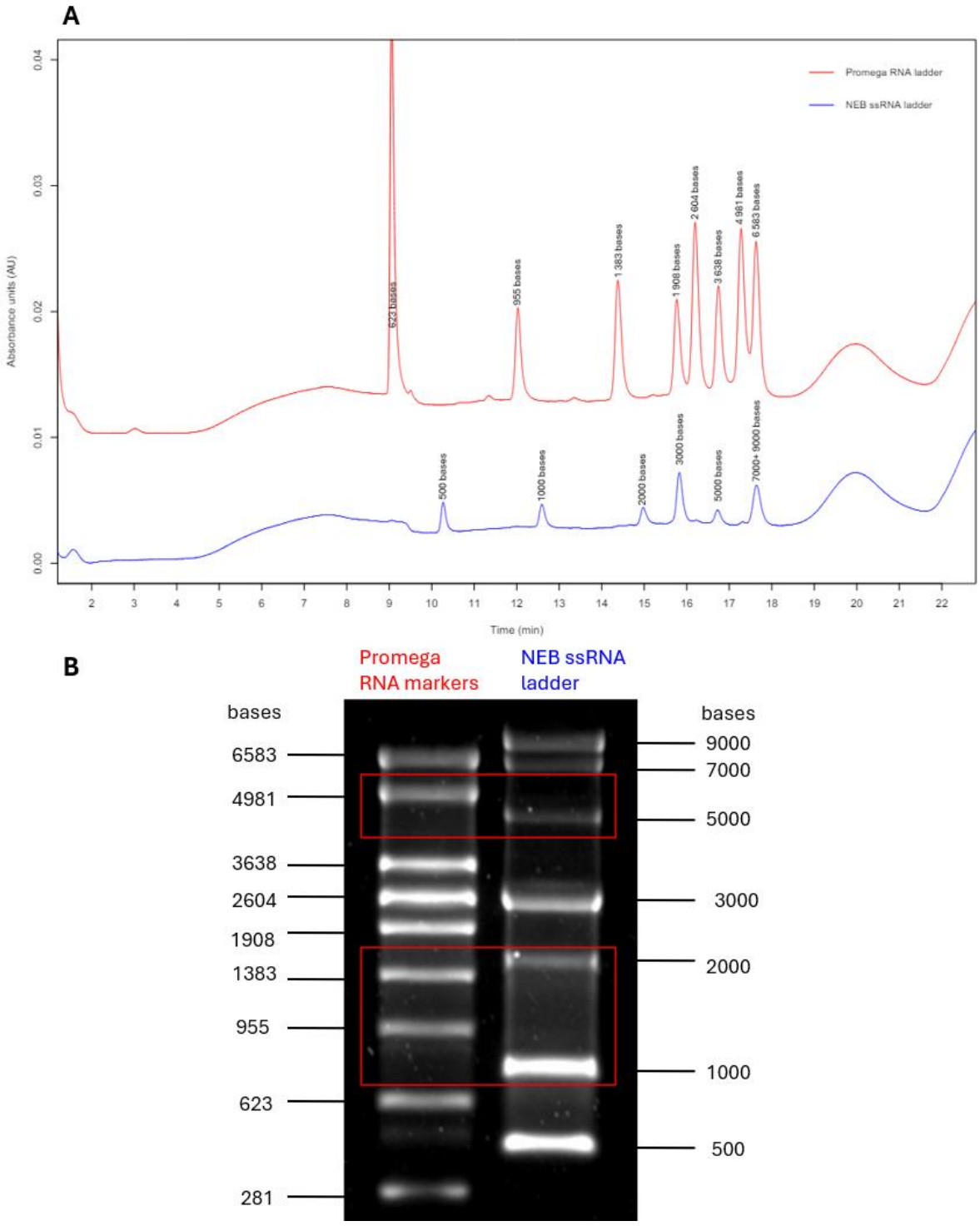

Figure 13. Analysis of Promega RNA markers (red) and NEB ssRNA ladder (blue) by IP-RP HPLC (A) and AGE (B). Ladder fragments do not align from the 1 kb to 5 kb region; an observation that is consistent across three different separation methods. Analyses by IP-RP HPLC were performed in triplicate (n = 3).

When the Promega RNA markers and NEB ssRNA ladder were analyzed by AGE and IP-RP HPLC a similar misalignment was observed, revealing that the misalignment of the RNA ladders is related to the RNA ladders themselves. RNA products can exhibit significant variability due to differences in their sequence composition, secondary structures, and interactions with the buffer system. Certain sequence compositions can promote the formation of secondary structures which can influence RNA migration through the gel matrix even under denaturing conditions (*73*).

2.4 Conclusion

Overall, the commercial kit separation method offers higher resolution and convenience compared to our in-house method and is particularly suitable for the analysis of mRNA products spanning a large size range (0.05 kb to 9 kb). However, for mRNA products, such as the COVID-19 vaccines, this extensive size range is not particularly necessary. One major limitation of using the commercial kit is its proprietary nature. The lack of transparency regarding buffer compositions and kit components makes troubleshooting challenging and complicates the ability to predict how the components may interact with mRNA products or influence their behaviors.

In contrast, the customization and control provided by in-house methods can address these issues, offering a tailored and flexible approach to RNA analysis. Developing an in-house CGE method offers better control over method parameters which can be optimized to achieve research needs. This flexibility is especially crucial to address the unique and evolving research surrounding mRNA therapeutics and allow for continuous progress. The ability to modify and fine-tune the method enhances the understanding of the technique and the different aspects that can influence results; a topic that will be further covered in the next

chapter. Ultimately, the level of control and adaptability provided by developing in-house methods is crucial for advancing RNA research and developing novel mRNA therapeutics, demonstrating the significant benefits of in-house over commercial CGE systems.

Misalignment of RNA ladders observed independently within each separation technique underscores the complexities associated with RNA products and the inherent difficulties in their analysis. These complexities of RNA analysis are further exacerbated by the variability in the separation media and conditions used across different techniques. For instance, capillary gel electrophoresis, agarose gel electrophoresis, and high-performance liquid chromatography each have unique separation mechanisms and matrix interactions that can differentially influence RNA migration. In the biotherapeutic context, where RNA integrity serves as a primary CQA, maintaining consistency and accuracy in RNA size determination is crucial. Therefore, a predictable reference standard is paramount. This standardization ensures that any variations observed in RNA integrity measurements are not due to methodological inconsistencies but rather reflect true changes in product quality.

3 A comprehensive evaluation of method parameters critical to the reliable assessment of therapeutic mRNA integrity by capillary gel electrophoresis

3.1 Background

In the previous chapter, we compared the performance of our in-house CGE-LIF method to an existing commercial kit for RNA analysis. We found that although the commercial kit offered higher resolution separation for the various ladders, the ability to fine-tune and optimize the performance of an in-house method is more valuable in the context of research.

With this in mind, we sought to explore various CGE-LIF method parameters to gain a better understanding of how they influence results and the measured mRNA integrity of mRNA-LNP drug products. Since instrument parameters have been previously explored (*71*), we decided to focus on the gel buffer composition as well as methods of LNP disruption. Additionally, a design of experiments (DOE) approach was taken to look at the interactive effects of gel additives and observe their impacts on measured mRNA integrity.

3.2 Materials and Methods

3.2.1 Reagents and samples

RNA markers (281 – 6583 b; G3191) was purchased from Promega Corporation (Wisconsin, USA). Nuclease-free Water (B1500L) was purchased from New England Biolabs (Massachusetts, USA). Reagents for CGE-LIF analysis were purchased from various vendors as previously indicated in chapter 2.2.1. Isopropanol (IPA; PX1834-1), and Triton X-100 (T9284) were purchased from MilliporeSigma (Missouri, USA).

A vendor product composed of mRNA (0.1 mg/mL; approximately 4200 bases in length) encapsulated in a mixture of PEGylated lipids (ALC-0159), ionizable lipids (ALC-0315), phospholipid 1,2-diasteroyl-sn-glycero-3-phosphocholine (DSPC) and cholesterol was used for the evaluation of LNP disruption methods and the DOE.

3.2.2 Lipid nanoparticle disruption and sample preparation

Prior to analysis, the Promega RNA markers were diluted to 0.025 mg/mL in 0.05X TBE and heat denatured at 70°C for 2 minutes then chilled on ice before being loaded into the instrument. LNP encapsulating mRNA were disrupted as follows: disruption by detergent was achieved by mixing 0.1 mg/mL of mRNA-LNP with a disruption solution containing either 2% or 20% Triton X-100 (w/w) in a 1:1 ratio (v/v) and incubating the mixture at 30°C while shaking at 600 rpm for 20 minutes. Isopropanol precipitation was achieved as previously described (*43*). For agarose gel electrophoresis, 0.3 µg of mRNA was mixed with RNA loading dye (2X) and heat denatured at 70°C for 2 minutes then cooled on ice for 5 minutes. For CGE-LIF analysis, 12 µL of disrupted mRNA was added to 132 µL of either 0.05X TBE or 0.05X TBE with 25% (v/v) formamide, heat-denatured at 70°C for 2 minutes and cooled on ice for 5 minutes.

3.2.3 AGE

AGE was performed as previously described in chapter 2.2.6 to evaluate the disruption of LNPs.

3.2.4 CGE-LIF instrumentation

CGE analyses were performed on a PA800 Plus Pharmaceutical Analysis System (AB Sciex) as previously described in chapter 2.2.3.

3.2.5 CGE-LIF analysis

CGE-LIF analysis was performed as previously described in chapter 2.2.5.

3.2.6 DOE set up and data analysis

For the DOE analysis, four different gel buffers were prepared as described above with adjustments made to urea concentration (2M or 6M) and dye concentration (0.005% (v/v) and 0.04% (v/v)). Samples containing formamide were prepared as described in section 0. A set of DOE analyses included two sequences designed to run eight different combinations (Table 3) of factors in duplicate (n = 32). The sequences were generated to account for day-to-day variability, and to assess order dependent effects by scrambling the run order. Three sets of DOE were performed to increase statistical power (n = 96). Peak integration was performed using the Empower 3 (version 7.21) software (Waters). Electropherograms were integrated into three areas: an early-migrating shoulder, the main peak, and a late-migrating smear (Figure A **1)**. Outliers were identified by calculating the percent difference the percent main peak area between replicates within a single sequence for each of the four sequences run (two sets); any combinations with a percent difference >20% was considered an outlier and was removed. A total of 20 runs were removed (n = 76). ANOVAs to examine factor-dependent effects were performed using RStudio (version 4.2.1). General linear models (GLM) were generated by Jun Gao with SAS® PROC GLMSELECT using a stepwise selection process.

Table 3. Eight DOE combinations and the associated conditions.

Combination #	Urea conc. (low or high)	Formamide	Dye conc. (% v/v)	Combination name
1	Low	Y	Low	1LYL
2	Low	Y	High	2LYH
3	Low	N	Low	3LNL
4	Low	N	High	4LNH
5	High	Y	Low	5HYL
6	High	Y	High	6HYH
7	High	N	Low	7HNL
8	High	N	High	8HNH

3.3 Results and Discussion

3.3.1 Effect of denaturants and gel additives on the separation of RNA by CGE-LIF in one-factor at a time experiments

In this study, we focused on gel buffer additives such as urea, formamide, and polyvinylpyrrolidone (PVP) since various instrument parameters have been explored elsewhere (*71*). One characteristic property of large RNA molecules is the propensity to form extensive secondary structures, which can interfere with accurate size-based separation (*73, 74*). Thus, common denaturants of RNA secondary structure such as urea and formamide are used to improve resolution of large mRNA molecules (*52*). With decreasing urea concentrations, RNA peaks were significantly broadened, and their electrophoretic mobility was increased (Figure 14A), reflecting previous reports (*73*). Urea acts as a nucleic acid denaturant by disrupting Watson-Crick base pairing and destabilizing secondary structure formation which can prevent dye molecules from being in the correct conformation (planar) to promote fluorescence (*75*). This is consistent with one past report suggested that urea significantly decreased fluorescence in CGE (*76*).

When formamide was added to samples prior to analysis, this seemed to increase variability and decrease signal intensity. Interestingly, the addition of formamide in-sample showed only minor improvements in peak resolution regardless of urea concentration (Figure 14B). Although formamide is commonly used to denature samples prior to analysis, the results suggested that its presence as a diluent is insufficient for significant denaturation by the time of analysis. Resolution was only improved when formamide was included in-gel (Figure 14C), which has been demonstrated by Lu *et al* (*52*). However, higher concentrations of in-gel formamide appear to abrogate fluorescence, possibly due to its impact on dye binding (*69*).

As the sieving polymer, PVP concentration is often adjusted based on the size of the analytes, with higher concentrations improving the resolution of larger fragments. Overall, increased PVP concentrations did improve resolution of larger fragments, albeit with reductions in overall intensity (Figure 14D).

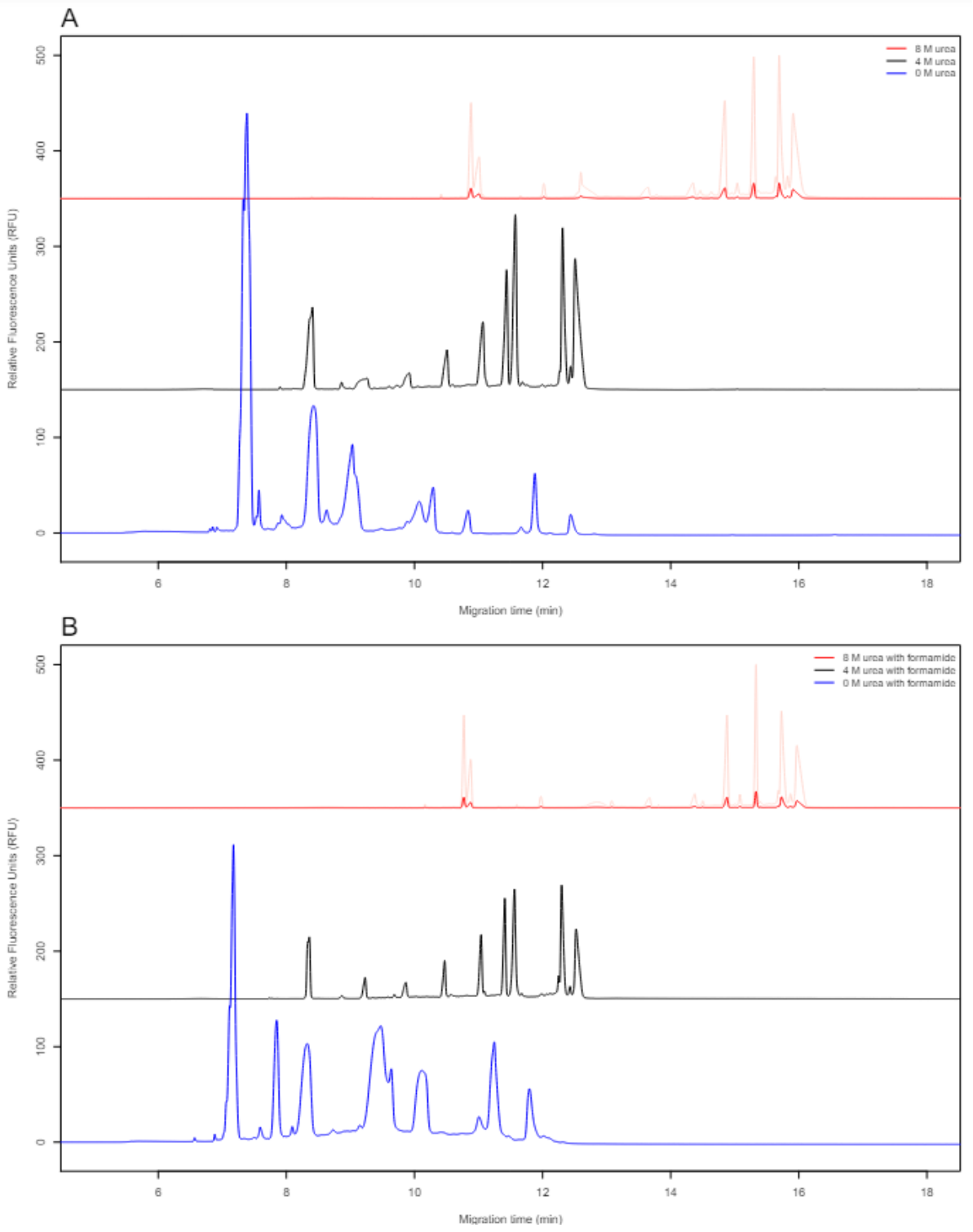
A
8 M urea
4 M urea
0 M urea
Relative Fluorescence Units (RFU)
0
100
200
300
400
500
6
8
10
12
14
16
18
Migration time (min)
B
8 M urea with formamide
4 M urea with formamide
0 M urea with formamide
Relative Fluorescence Units (RFU)
0
100
200
300
400
500
6
8
10
12
14
16
18
Migration time (min)

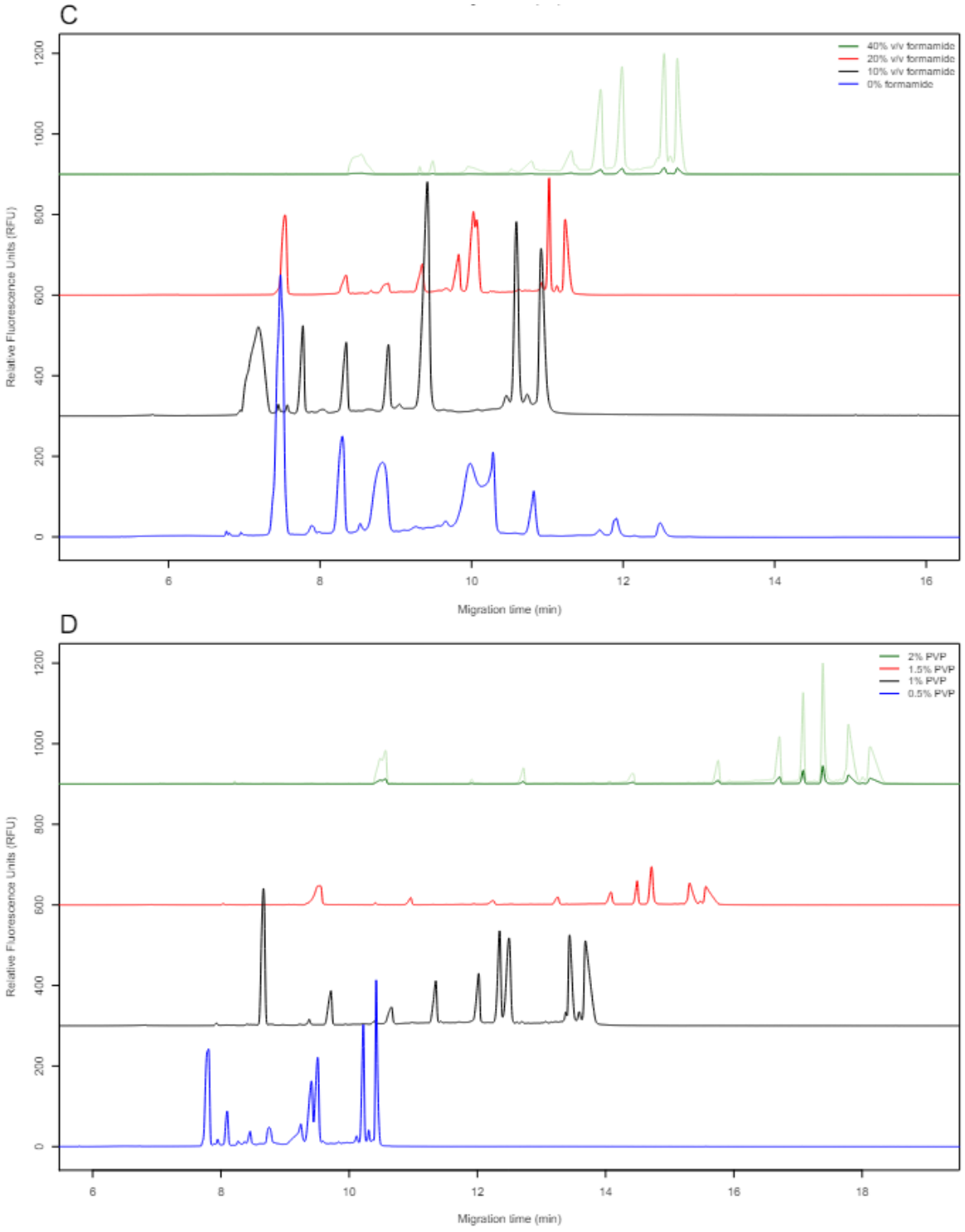

Figure 14. CGE-LIF traces of Promega RNA markers in various change one factor at a time experiments. Decreasing urea concentrations results in peak broadening in the absence (A) and presence (B) of formamide in the sample buffer. Formamide in the sample buffer (B) does not appear to significantly increase the resolution; however, formamide added directly to the gel buffer (C) does to an extent. Increasing PVP concentration (D) in the gel buffer slightly improves the resolution of larger fragments. Light coloured traces are the same as

their respective colours but with intensities normalized to improve visualization of the low-intensity peaks. CGE-LIF analyses were performed in triplicate (n = 3).

3.3.2 Separation of mRNA-LNP samples and quantification of disruption efficiency

In order to analyse mRNA quality in most biotherapeutic products, the stable and protective encapsulating LNP needs to be disrupted. Only extracted and free mRNA molecules can be evaluated by CGE-LIF. After disruption, the free mRNA profile can be visualized as a single sharp peak, the intact material, and a broad earlier-eluting shoulder (*49*), which contains mRNA fragments caused by the production or encapsulation process.

Since CGE-LIF is a method that depends on dye-binding to mRNA to produce a signal, LNPs encapsulating the mRNA must be disrupted prior to analysis. A common method seen in literature is a detergent-based disruption that uses Triton X-100 or similar reagent (*66, 69*). Another method, used by Packer *et al.*, is an isopropanol precipitation where mRNA is precipitated and spun into a pellet that is reconstituted in NFW (*43*).

When an mRNA-LNP biotherapeutic was disrupted by Triton X-100, the overall fluorescence signal was strongly impacted, even at low concentrations (1%), while isopropanol precipitation produced the highest signal (Figure 15A). In addition, treatment with Triton X-100 influenced the relative area of the main peaks compared to the shoulder (Table 4). When the disruption treatments were applied to an RNA ladder, a similar trend was observed (Figure 15B), suggesting that the removal of non-precipitating buffer components improves assay sensitivity. Interestingly, when RNA samples were treated and analyzed by agarose gel electrophoresis, high detergent concentrations appeared to disrupt

the electrophoretic mobility of RNA, causing faint bands and streakiness (Figure 16). This was observed in both control RNA and disrupted mRNA-LNP samples.

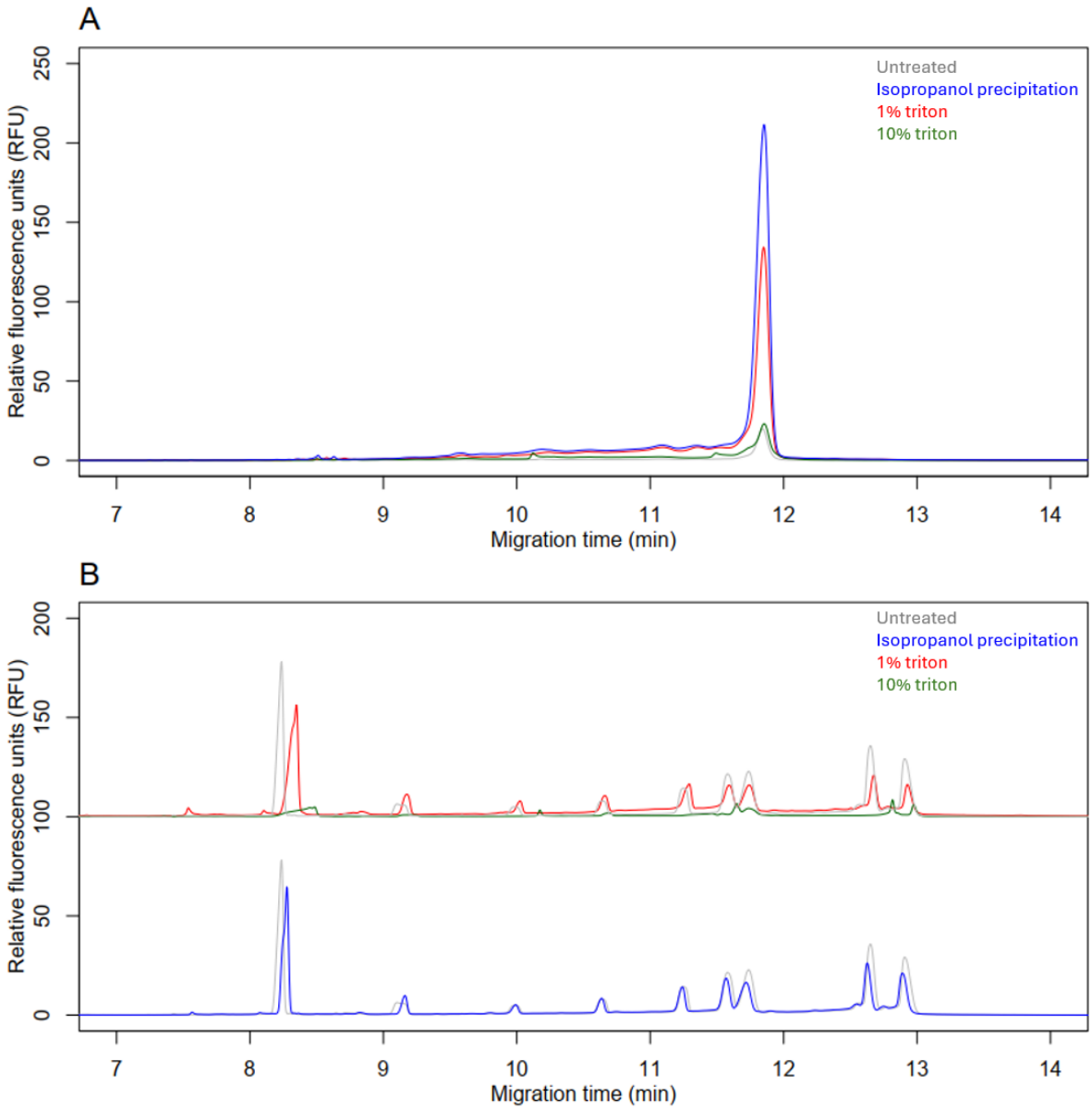

Figure 15. Impact of LNP disruption method on CGE-LIF signal intensity. mRNA-LNP samples analyzed by CGE-LIF after LNP disruption (A) and Promega RNA markers mock disrupted with the same disruption protocols (B). Treatment with Triton X-100 appears to impact the overall fluorescence signals by CGE-LIF. Untreated sample trace was duplicated and stacked to improve visualization. CGE-LIF analyses were performed in triplicate (n = 3).

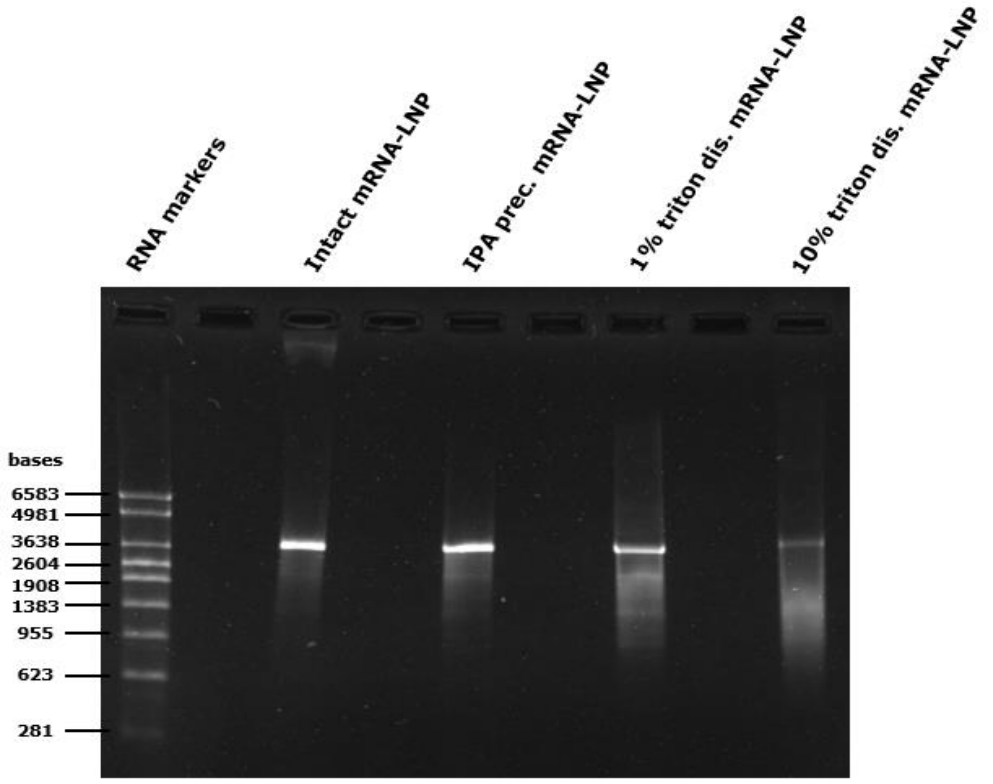

Figure 16. Verification of LNP disruption by agarose gel electrophoresis. The intact mRNA-LNP lane contains a sharp band that corresponds with the expected size of the mRNA product and a larger unresolved band that is not observed in the lanes containing disrupted samples. The presence of detergent appears to disrupt the electrophoretic mobility of RNA resulting in streaking.

Since isopropanol precipitation did not appear to strongly influence fluorescence intensity (Figure 15), this method of sample preparation was chosen for the disruption of mRNA-LNPs.

Table 4. Peak area (%) composition of mRNA-LNP samples disrupted using different protocols. Values were calculated based on the average of triplicates (n = 3).

Disruption Method	Shoulder Avg % peak area	Main peak Avg % peak area	Late migrating smear Avg % peak area
Isopropanol precipitation	39.42	55.42	5.16
1% Triton X-100	50.77	43.39	5.84
10% Triton X-100	76.67	10.59	12.74

3.3.3 Design of experiments approach to systematically evaluate interactive effects of method parameters that influence CGE-LIF method performance

One recurring observation was the impact of sample and gel additives on peak signal and variability of peak profiles. In particular, urea and formamide are ubiquitous in RNA analysis and their usage can vary greatly depending on the method (*52*, *73*), potentially impacting interpretation of results. Lower urea concentrations could bias relative peak intensities and increasing formamide could hinder run-to-run reproducibility. In addition, both additives reduced the overall peak signals, potentially impacting fluorescent dye binding to RNA. Since the shoulder profile containing mRNA fragments is significantly lower than the main peak, a lower signal-to-noise ratio could present problems for consistent or accurate integration (*77*).

Given the complexity and potential for interplay between urea, formamide, and dye, a structured and systematic DOE was carried out to examine factor effects. Three factors were chosen (urea concentration, addition of formamide to the sample, and concentration of dye) at 2 levels each (Table 5), for a 2^3 full factorial design. Two sequences were constructed, with randomized orders (Figure 17). The overall time of each sequence was less than 9 hours in order to minimize the sample 4°C storage time in the autosampler. Longer storage times impacted peak intensities due to the sensitive nature of RNA (Figure 18). Both sequences were repeated as a set to increase statistical power (n = 64).

Table 5. Factors and levels in the full factorial design. Three factors chosen to be evaluated at two levels each.

Factor	Levels	
Urea	Low (2M)	High (6 M)
Formamide	No	Yes
Dye	Low (0.005% v/v)	High (0.04% v/v)

Sequence 1 (Day 1)

Run #	Time (mins)	Combination ID	Urea conc.	Formamide	Dye conc.
1	25	1	Low (2M)	Yes	Low(0.5X)
2	50	5	High (6M)	Yes	Low(0.5X)
3	75	3	Low (2M)	No	Low(0.5X)
4	100	7	High (6M)	No	Low(0.5X)
5	125	2	Low (2M)	Yes	High (4X)
6	150	6	High (6M)	Yes	High (4X)
7	175	4	Low (2M)	No	High (4X)
8	200	8	High (6M)	No	High (4X)
9	225	1	Low (2M)	Yes	Low(0.5X)
10	250	5	High (6M)	Yes	Low(0.5X)
11	275	3	Low (2M)	No	Low(0.5X)
12	300	7	High (6M)	No	Low(0.5X)
13	325	2	Low (2M)	Yes	High (4X)
14	350	6	High (6M)	Yes	High (4X)
15	375	4	Low (2M)	No	High (4X)
16	400	8	High (6M)	No	High (4X)

Sequence 2 (Day 2)

Run #	Time (mins)	Combination ID	Urea conc.	Formamide	Dye conc.
1	25	8	High (6M)	No	High (4X)
2	50	4	Low (2M)	No	High (4X)
3	75	6	High (6M)	Yes	High (4X)
4	100	2	Low (2M)	Yes	High (4X)
5	125	7	High (6M)	No	Low(0.5X)
6	150	3	Low (2M)	No	Low(0.5X)
7	175	5	High (6M)	Yes	Low(0.5X)
8	200	1	Low (2M)	Yes	Low(0.5X)
9	225	8	High (6M)	No	High (4X)
10	250	4	Low (2M)	No	High (4X)
11	275	6	High (6M)	Yes	High (4X)
12	300	2	Low (2M)	Yes	High (4X)
13	325	7	High (6M)	No	Low(0.5X)
14	350	3	Low (2M)	No	Low(0.5X)
15	375	5	High (6M)	Yes	Low(0.5X)
16	400	1	Low (2M)	Yes	Low(0.5X)

Figure 17. Two sequences constructed to test 8 combinations of factors in a randomized order. Replicates within a sequence control for time-dependence effects. Running the sequence on different days controls for day-to-day variability and the scrambled sequence controls for order-dependence effects.

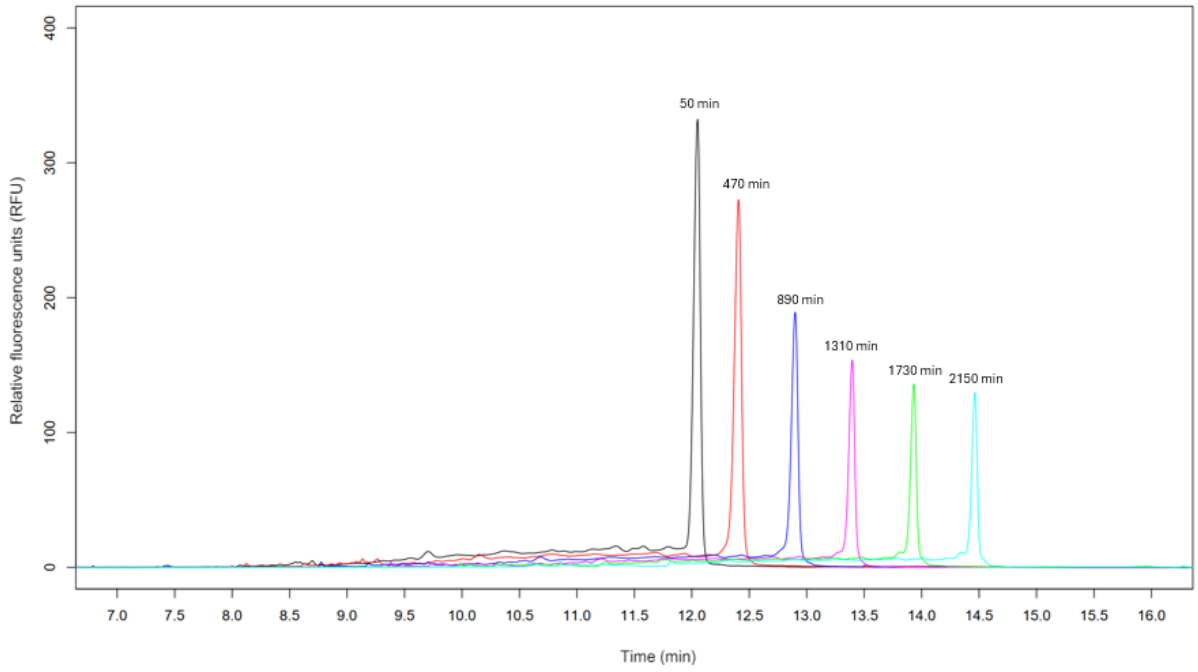

Figure 18. CGE-LIF traces of disrupted mRNA-LNP samples over the course of 36 hours in the auto-sampler. Peak intensity decreases over time and appears to plateau after approximately 29 hours.

The resulting electropherograms (Figure 19) were integrated into three areas: the early-migrating shoulder, the main mRNA peak, and any late-migrating smear. Box plots of the main peak percentage within each condition (Figure 20) showed that variability was highest when all factors were at their lowest levels and highest levels. Interestingly, the conditions with the lowest urea consistently resulted in the highest main peak percentage or integrity. As seen in Figure 19, all combinations with low urea (top row) show a compact shoulder relative to the combinations with high urea (bottom row). This along with the observations from chapter 3.3.1 (Figure 14A) suggests that low concentrations of urea may result in an inflated integrity measurement due to the poor resolution between the early-migrating shoulder and the main peak.

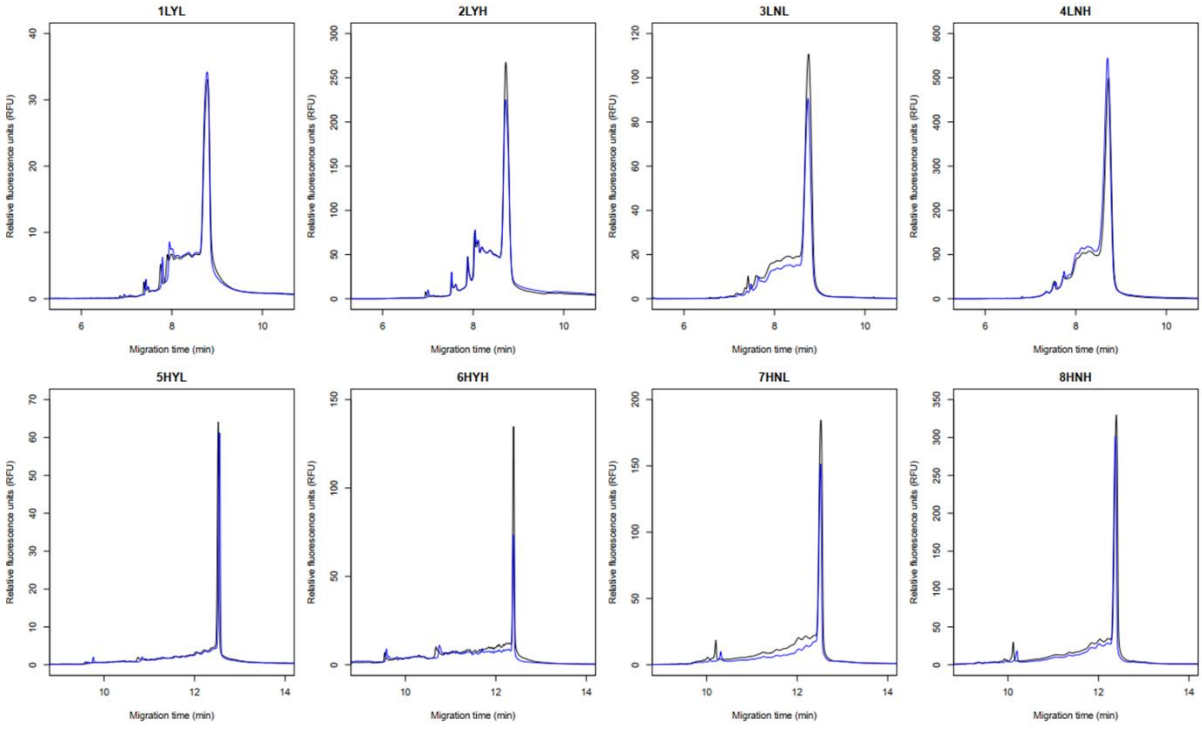

Figure 19. Electropherograms of each of the 8 combinations of conditions for one set (two sequences) of analyses. High urea conditions (bottom row) appear to better separate the shoulder region from the main peak (bottom row). Under low urea conditions (top row) the shoulder appears more compact. The full DOE experiment was performed thrice (n = 96).

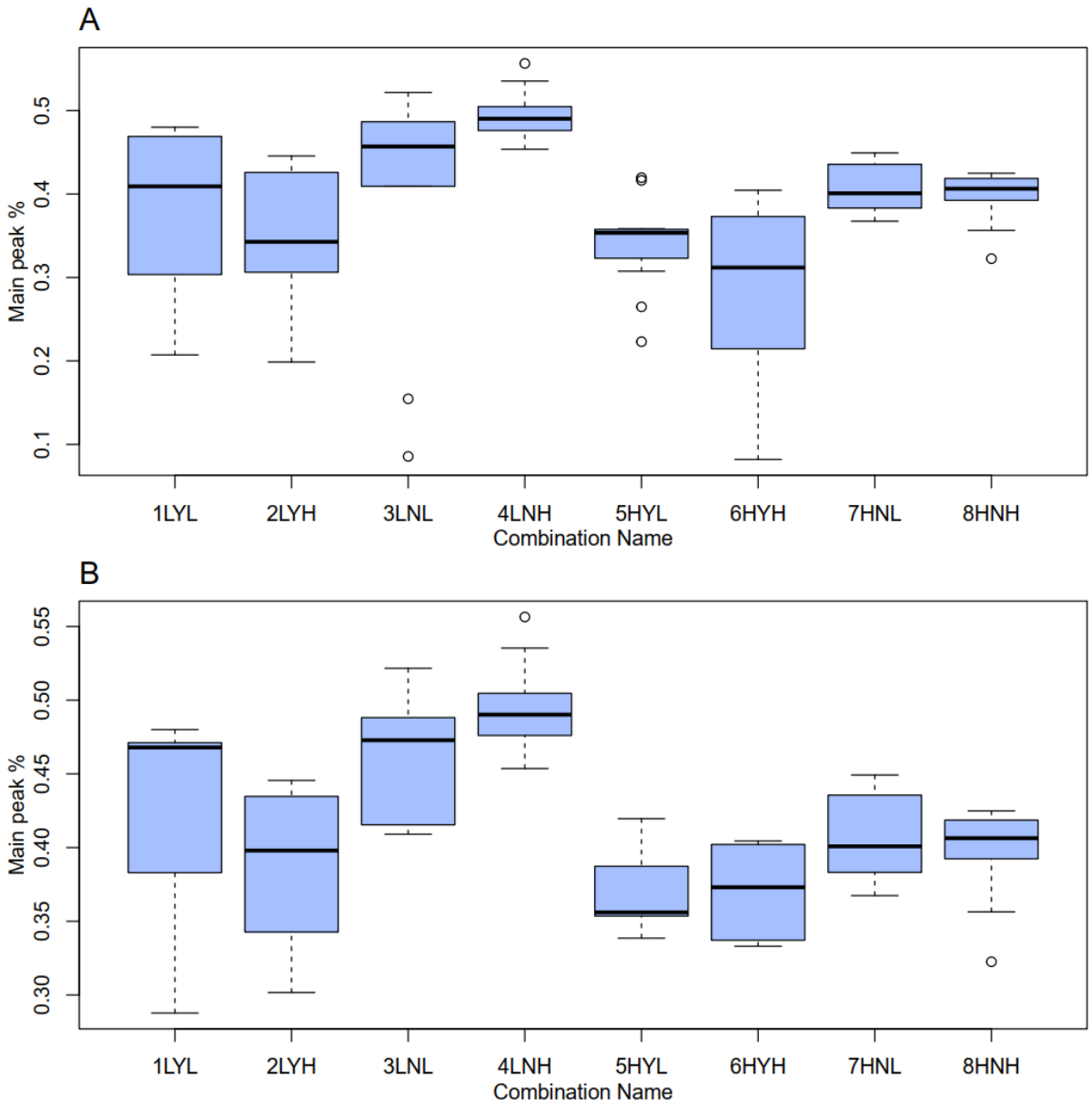

Figure 20. Box plots of mRNA main peak percentages for each condition. Combination names and the associated conditions are as indicated in

Table **3**. The top panel (A) shows the variability before outlier removal (n = 96), and the bottom panel (B) after outlier removal (n = 76). Low urea conditions consistently show higher main peak percentages/integrity measurements than high urea conditions.

An examination of factor-dependent effects by GLM (Table 6) showed that the combination of urea concentration and formamide was significantly correlated with the main peak percentage, with low urea concentration and absence of formamide resulting in a larger main peak area. Interestingly, the shoulder percentage was also significantly impacted by changing urea conditions which supported prior observations that urea concentration disproportionately impacted fragments based on size. The addition of formamide appeared to impact the late-migrating smear percentage, suggesting that the variability associated with formamide addition could be caused by peak tailing.

Table 6. GLMSELECT Stepwise selection model. In stepwise selection, effects are iteratively added and/or removed. If at any step in the method, any effect in the model is considered to be not significant, the least significant effect is removed from the model before it proceeds to the next step. This iterative approach ensures that a new effect cannot be added to the model if an existing one is deemed insignificant, decreasing the likelihood of misattributing significance **(*78*)**.

Main peak percentage					
Parameter	DF	Estimate	Standard Error	t value	Pr > |t|
Intercept	1	39.516230	0.603920	65.43	<0.0001
urea_conc*formamide 2 0	1	8.471641	1.122470	7.55	<0.0001
Shoulder percentage					
Parameter	DF	Estimate	Standard Error	t value	Pr > |t|
Intercept	1	55.647895	0.698129	79.71	<0.0001
urea_conc 2	1	-6.964474	0.987303	-7.05	<0.0001
Late-migrating smear percentage					
Parameter	DF	Estimate	Standard Error	t value	Pr > |t|
Intercept	1	9.188667	0.668824	13.74	<0.0001
formamide 0	1	-5.490841	0.859686	-6.39	<0.0001

3.4 Conclusion

High-resolution analysis of large mRNA molecules can be challenging by CGE-LIF. The propensity for mRNA to form extensive secondary structure produces many conformers,

which are difficult to separate. The susceptibility of large mRNA molecules to hydrolyze at random positions also limits acceptable experimental conditions. Several groups have evaluated methods to analyse purified RNA, although the majority of these were developed for research applications in mind (*49, 59, 70*). Since mRNA drug substances are complex mixtures containing various sizes and impurities, it is important to understand which parameters would have the highest impact on the quality assessment.

While DOE is often used for the optimization of desired outputs or responses, it can also be a valuable tool to identify interactions that could be missed with one factor at a time experiments (*79*). The results of our one factor at a time and DOE experiments revealed that mRNA integrity results by CGE-LIF are extremely sensitive to method parameters. For example, varying urea conditions evidently influences the integrity measurement – with low urea conditions contributing to a higher mean peak percentage. Therefore, maintaining a tight control on urea conditions is important. Common errors such as not taking the volume of urea salt into account would not be acceptable batch-to-batch. Furthermore, using higher urea concentrations avoids inflating the integrity percentage by improving the separation between the shoulder and the main peak. The results also reveal that while formamide is not necessary to include in the diluent, it can be used to improve resolution when added directly to the gel buffer. Ultimately, integrity values between different methods cannot be compared and it is abundantly clear that standardization is necessary to be able to appropriately compare mRNA products head-to-head.

4 A comparative analysis of capillary gel electrophoresis and ion-pair reversed phase liquid chromatography for the assessment of mRNA therapeutics

4.1 Background

While mRNA is well-understood as a research tool, its complexities as a biotherapeutic product are still being explored. Indeed, one critical quality attribute of interest is integrity. Currently, two analytical methods dominate mRNA integrity assessments: capillary gel electrophoresis (CGE) and ion-pair reverse phase liquid chromatography (IP-RPLC). The two techniques operate on significantly different separation mechanisms which suggests that the impurity profile measured may also differ; therefore, the orthogonality of these methods should be examined.

The lack of consensus, available data, and reference standards make product-to-product assessments difficult. To address this gap, our lab evaluated and compared CGE and IP-RPLC for mRNA integrity analysis with the aim of clearly defining differences between methods.

4.2 Materials and Methods

4.2.1 Reagents and samples

RNA markers (281 – 6583 b; G3191), Luciferase Control RNA (1803 b; L4561), and Kanamycin Positive Control RNA (1.2 kb; C1381) were purchased from Promega Corporation (Wisconsin, USA). Reagents for CGE-LIF analysis, IP-RP HPLC analysis and LNP disruption were purchased from various vendors as previously indicated in chapters 2.2.1 and 3.2.1.

A vendor product composed of mRNA (0.1 mg/mL; approximately 4200 bases in length) encapsulated in a mixture of PEGylated lipids (ALC-0159), ionizable lipids (ALC-0315), DSPC and cholesterol was used to evaluate method performance.

4.2.2 LNP disruption and sample preparation

Promega RNA markers and vendor mRNA-LNP were prepared as described in chapter 3.2.2. Luciferase Control RNA was diluted to 0.025 mg/mL in 0.05X TBE; both the diluted Promega RNA markers and the Luciferase Control RNA were spiked with the Kanamycin Positive Control RNA (0.005 mg/mL). For IP-RPLC analysis, disrupted mRNA and commercial RNA were diluted to the same concentration as CGE-LIF in NFW before injection.

4.2.3 Instrumentation

CGE analyses were performed on a PA800 Plus Pharmaceutical Analysis System (AB Sciex) and IP-RPLC analyses were performed on a Waters Alliance e2695 Separation Module (Waters) as previously described in chapter 2.2.3.

4.2.4 CGE-LIF analysis

CGE-LIF analysis was performed as previously described in chapter 2.2.5.

4.2.5 IP-RP HPLC

An adapted method was used for available instrumentation (*43*). Flow rate was maintained at 0.35 mL/min and a column temperature of 60°C was used. Mobile phase A consisted of 50 mM DBAA, and 100 mM TEAA and mobile phase B consisted of 50% acetonitrile, 50 mM DBAA, and 100 mM TEAA. 10 µL of sample (approximately 40 ng of mRNA) was injected

for each analysis, and mRNA was detected by UV at 260 nm. Data acquisition and analysis were performed using the Empower 3 (version 7.21) software (Waters).

4.2.6 Electropherogram integration and data analysis

Peak integration was performed using the Empower 3 (version 7.21) software (Waters). Electropherograms were integrated into three areas: an early-migrating shoulder, the main peak, and a late-migrating smear (Figure A 1).

4.3 Results and Discussion

4.3.1 Evaluation of method performance

To compare the performance of CGE to IP-RPLC, a method described by Packer et al., (*43*) was implemented. Luciferase Control RNA spiked with the Kanamycin Positive Control RNA internal standard (IST; marked by an asterisk) was analyzed alongside a nine-fragment RNA marker (Figure 21). Chromatogram quality served as the basis for method performance assessment, focusing on RNA marker linearity, resolution factors and accuracy in determining RNA size (Table 7). The resolution factors between the IST and luciferase RNA peak showed that CGE offers higher resolution than IP-RPLC. Similar to the observations regarding the relationship between migration time and RNA length described in chapter 2.3.1, we noticed that the linearity of the RNA markers again exhibit a biphasic trend (Figure 22). When the RNA marker fragments were considered as two separate populations (low and high molecular weight) the resolution factors indicated that CGE offers better separation and resolution across the entire fragment range. The low resolution of IP-RPLC, particularly for higher molecular weight (>2.5 kb) fragments, made it difficult to precisely determine RNA length. For instance, the overlaid luciferase peak elutes in the region between the 1.9 kb and

2.6 kb fragments, and the poor resolution compromises the precision when determining fragment size resulting in a higher % error in size determination.

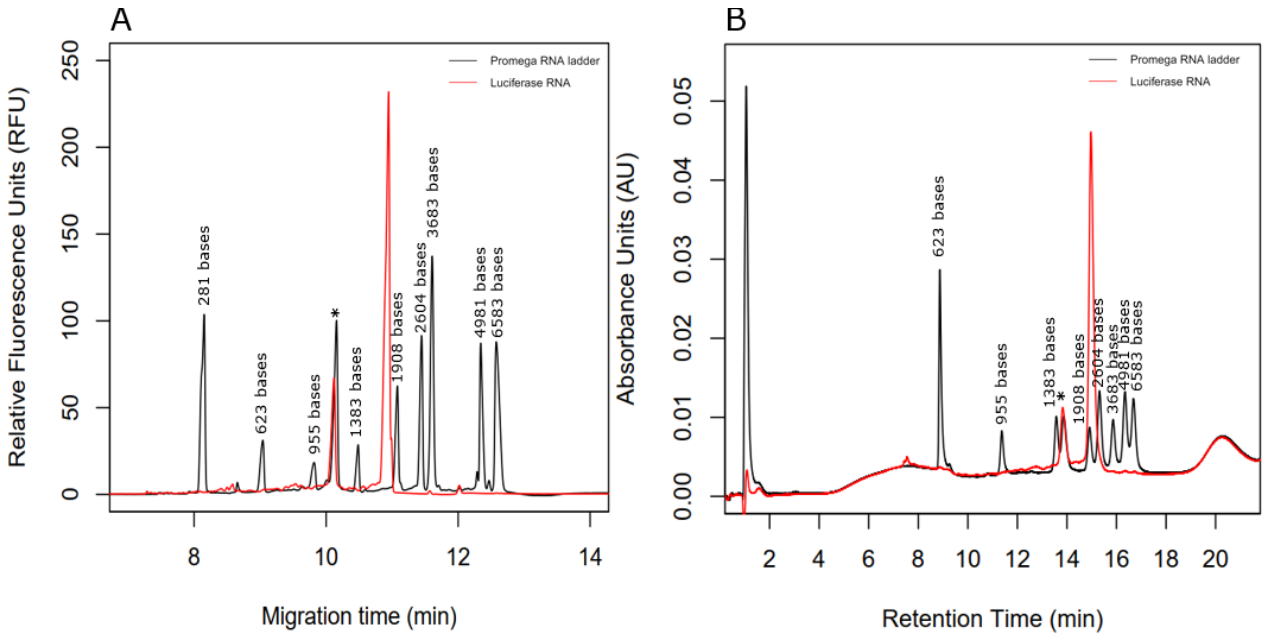

Figure 21. Luciferase RNA spiked with IST analyzed by CGE-LIF (A) and IP-RP HPLC (B). Luciferase Control RNA (red) was analyzed alongside RNA markers (black); both were spiked with a 1.2 kb IST (*). Analyses were performed in triplicate (n = 3) for each technique.

Table 7. Summary of quantitative values used to compare chromatogram quality. Values were calculated based on the average of triplicates (n = 3).

Method	Linearity of RNA markers (R^2)			Resolution Factor (Rs)			Calculated size of Luciferase RNA (bases)	% difference of calculated size
	Full Range	Low MW range	High MW range	Between 623 and 955 peaks	Between 3638 and 4981 peaks	Between IST and control RNA		
CGE	0.990	0.968	0.936	6.12	5.0	3.26	2074	6.04
IP-RPLC	0.883	0.929	0.963	5.00	1.08	1.45	2783	46.28

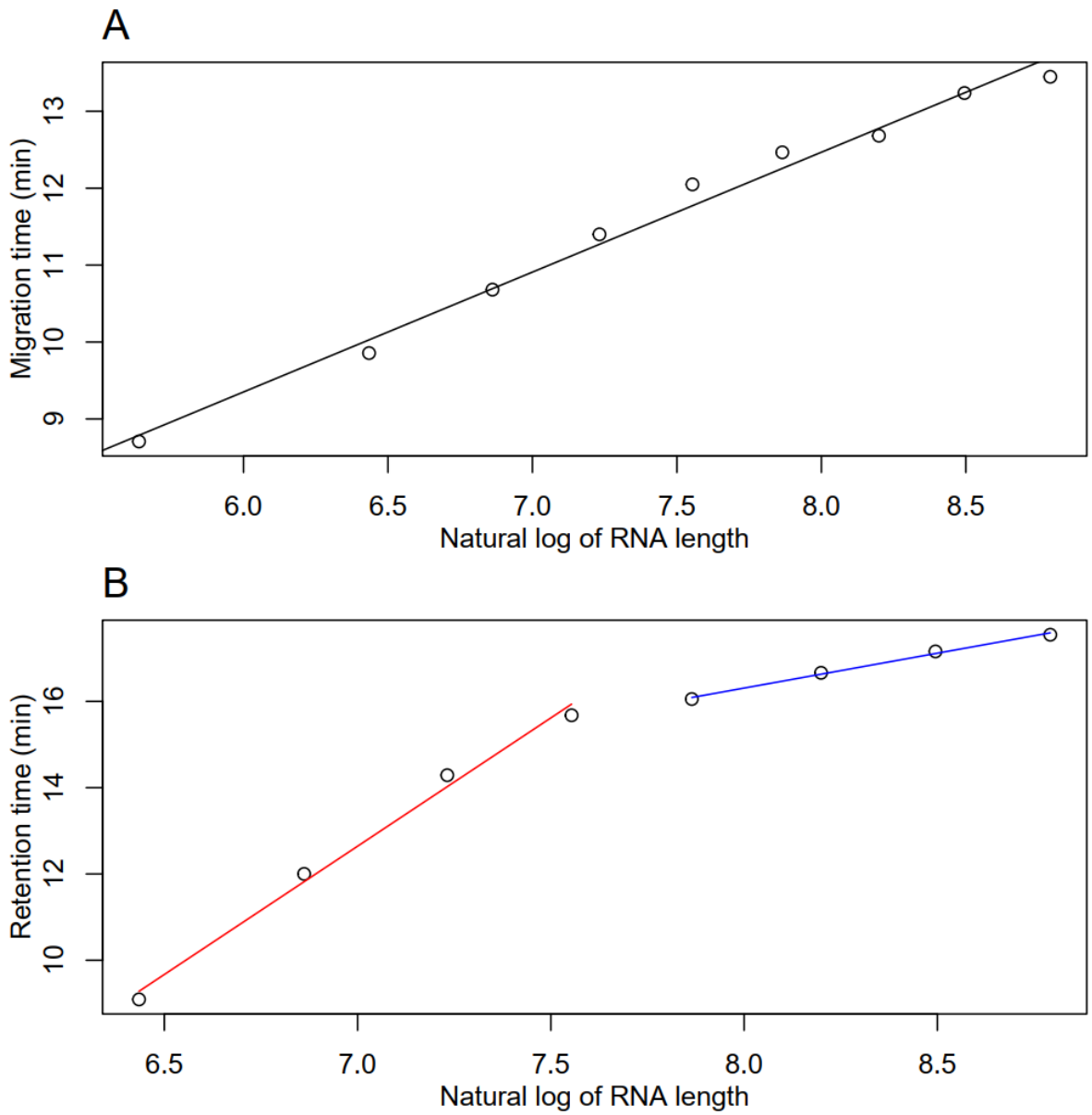

Figure 22. Linear and biphasic relationship between migration time and RNA length by CGE-LIF and IP-RP HPLC. The linearity of the Promega ladder by CGE-LIF (A) and IP-RP HPLC (B) exhibit biphasic linearity with a breakpoint of approximately 2 kb. The red line is fitted up to fragments with lengths up to 2 kb, and the blue to fragments above 2 kb. Analyses were performed in triplicate (n = 3) for each technique.

4.3.2 Integrity analysis of mRNA-LNP samples

When mRNA-LNP samples were analyzed (Figure 23), similar observations regarding resolution could be made. While a main peak is evident by both methods, CGE also reveals a clear shoulder caused by the presence of truncated RNA and related impurities. This

shoulder is not as well resolved from the main peak by IP-RPLC. Integration values were also different (Table 4 and Table 8). IP-RPLC values were consistently higher, potentially due to its lower resolving power and broader peaks compared to CGE. This broadening effect may obscure similarly sized fragments within the main peak, inflating the integrity value.

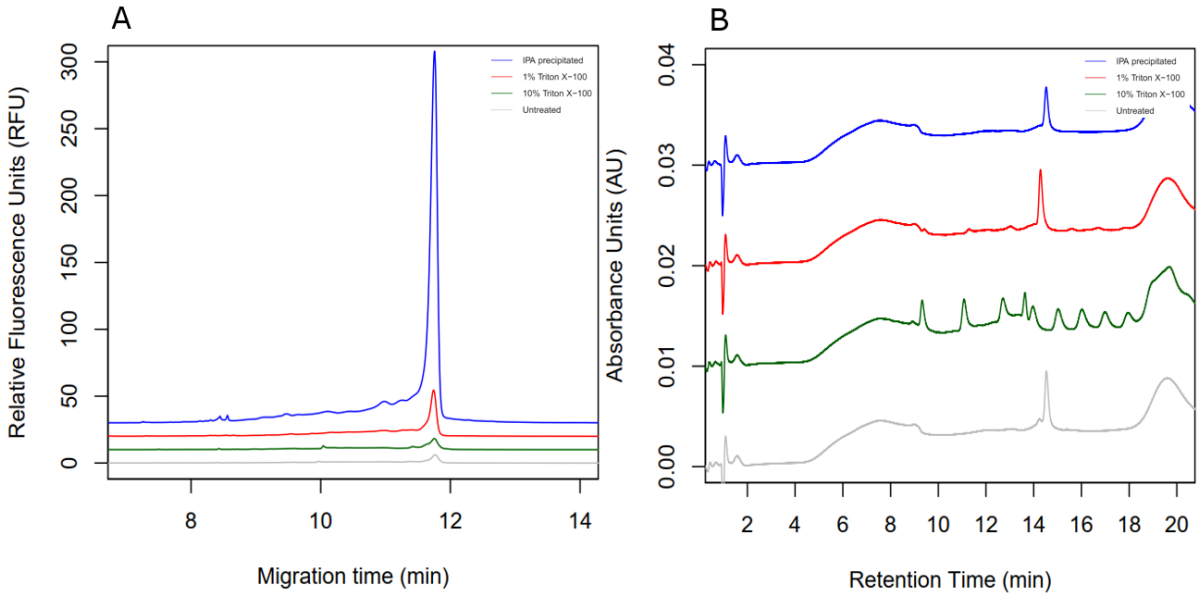

Figure 23. mRNA-LNP samples analyzed by CGE-LIF (A) and IP-RP HPLC (B). High concentrations of Triton X-100 (>10%) interfere with the UV detection of mRNA at 260 nm. Analyses were performed in triplicate (n = 3).

Table 8. Peak area (%) composition of mRNA-LNP samples disrupted using different protocols analyzed by IP-RPLC. Values were calculated based on the average of triplicates (n = 3).

Disruption Method	Shoulder Avg % peak area	Main peak Avg % peak area
No disruption	23.24	76.76
Isopropanol precipitation	19.28	80.72
1% Triton X-100	17.88	82.12
10% Triton X-100	N/A	N/A

The mRNA-LNP analyses also highlight the impact of disruption methods on results, underscoring the critical role of sample preparation in obtaining accurate and reliable data. For instance, IP-RPLC analysis of an mRNA-LNP sample disrupted with 10% triton reveals interference due to triton's overlapping absorbance spectrum with mRNA (*80*). This can potentially skew absorbance readings, masking or distorting the true signal of mRNA. This highlights how the choice technique along with disruption methods can yield different impurity profiles, directly influencing the quality and interpretability of analytical results. Similarly, CGE results are affected by disruption methods, with sample matrix influencing signal intensities. The concentration of triton in the sample matrix alters the signal intensities, leading to signal suppression. This potentially results in inaccurate quantification and misleading conclusions regarding the integrity of mRNA products.

These observations illustrate the broader principle that sample preparation is a crucial determinant of analytical outcomes and interpretability of results. In addition to the choice of analytical technique, choice of disruption methods, buffers, and other preparative steps must be scrutinized to appropriately compare products head-to-head. Therefore, in the context mRNA therapeutics, understanding and appropriately controlling the impact of method parameters is vital to inform standardization of practices and analytical techniques. By establishing standardized protocols, the reliability of analyses will be enhanced – leading to more robust development and quality control of mRNA-based therapeutics.

4.4 Conclusion

Although both CGE and IP-RP HPLC can be used to assess mRNA integrity, our studies have shown that they are not interchangeable, and each have unique advantages and disadvantages. By shedding light on these limitations, we hope to support the development of

appropriate methods and standards. It is fundamental to understand the advantages and limitations of each technique to be able to accurately assess and compare products and achieve standardization of assessment.

5 Protection of mRNA payloads by LNP and the thermal stability of mRNA-LNP

5.1 Background

Central to the success of mRNA-based therapies is their stability, which directly impacts their efficacy, safety, and shelf life. Ensuring the stability of mRNA therapeutic products is crucial, as instability can lead to degradation of the mRNA molecules, loss of therapeutic potency, and potential immunogenicity issues (*32*, *81*, *82*). A critical innovation in enhancing the stability of mRNA vaccines is the use of LNPs. LNPs encapsulate the mRNA, conferring protection against enzymatic degradation and physical stress during storage and delivery. LNP encapsulation not only improves the stability of mRNA but also facilitates the efficient delivery into target cells – enhancing the overall product effectiveness (*34*).

Given the complexity and sensitivity of mRNA molecules, rigorous stability testing is imperative to meet regulatory requirements and to guarantee the quality and consistency of mRNA therapeutics (*22*). This involves both real-time and accelerated stability studies to predict the shelf life and optimal storage conditions of these products. Moreover, stability data guide the development of formulation strategies and the design of delivery systems that protect mRNA from degradation. Monitoring the stability of mRNA therapeutics involves a comprehensive understanding of the factors that influence RNA integrity, including temperature, pH, enzymatic activity, and the presence of impurities. Analytical techniques are employed to assess the stability profile of mRNA products, ensuring that they maintain their structural and functional integrity from production through to delivery to patients (*83*).

In this context, the importance of monitoring the stability of mRNA therapeutic products cannot be overstated. It is a critical aspect of the development process that ensures the reliability and success of mRNA-based interventions, ultimately contributing to the advancement of precision medicine and the improvement of patient outcomes.

5.2 Materials and Methods

5.2.1 Reagents and samples

Reagents for CGE-LIF analysis and LNP disruption were purchased from various vendors as previously indicated in chapter 3.2.1.

The mRNA-LNP samples used for this thermal stability study were kindly gifted by Dr. Michael Johnston (Nanomedicine laboratory, Health Canada). The samples consist of firefly luciferase RNA (FLuc) encapsulated in one of three lipid formulations as follows: 1) KC2 cationic ionizable lipids: DSPC: cholesterol: 1,2-dimyristoyl-rac-glycero-3-methoxypolyethylene glycol-2000 (DMGPEG-2000) (% molar ratio; 50:10:38.5:1.5), 2) SM102 cationic ionizable lipids: DSPC: cholesterol: DMGPEG-2000 (% molar ratio; 50:10:38.5:1.5), and 3) ALC-0315 cationic ionizable lipids: DSPC: cholesterol: ALC-0159 pegylated lipids (% molar ratio; 46.3:9.4:42.7:1.6). Prior to receipt, these samples were stored at either 4°C, room temperature (23°C), or 37°C for three weeks. Upon receipt, the samples were stored in their respective conditions (as indicated) for two weeks before all were moved to -80°C.

5.2.2 LNP disruption and thermal stability study

For each of the three FLuc mRNA samples encapsulated in different lipid formulations, the LNPs encapsulating the payloads were disrupted using the isopropanol precipitation as

described in chapter 3.2.2. A thermal stability study test was conducted by extracting FLuc mRNA from the LNP and incubating the samples at -80°C, 4°C, and at room temperature (RT) for four weeks. Each week an aliquot was taken and analyzed by CGE-LIF to monitor integrity and fragmentation. Since previous CGE-LIF analyses (chapter 3.2.1) were performed with ALC-0315 containing LNP formulations, a comparable formulation was chosen for the FLuc mRNA stability studies.

5.2.3 CGE-LIF instrumentation

CGE analyses were performed on a PA800 Plus Pharmaceutical Analysis System (AB Sciex) as previously described in chapter 2.2.3.

5.2.4 CGE-LIF analysis

CGE-LIF analysis was performed as previously described in 2.2.5.

5.2.5 Electropherogram integration and data analysis

Peak integration was performed using the Empower 3 (version 7.21) software (Waters). Electropherograms were integrated into two areas: an early-migrating shoulder, and the main peak (Figure A 1).

5.3 Results and Discussion

5.3.1 Protective effect of LNP on mRNA

The first set of preliminary experiments revealed that LNP encapsulation of mRNA conferred significant protection against thermal degradation at 4°C. We found that mRNA encapsulated in LNP remained stable and intact upon disruption and CGE-LIF analysis even after more than five weeks of storage at 4°C (Figure 24, magenta trace). This mRNA sample had a main peak percentage of approximately 55.9% (

Table 9), which is comparable to integrity values measured for the product (Table 4). These observations regarding stability are similar to the ones made by Tong *et al*., (*64*) where they demonstrated mRNA integrity remains stable for up to 3 months at 4°C when it remains encapsulated in LNPs. However, after the LNP of the same sample is disrupted and stored under the same 4°C conditions, mRNA quickly degrades with significant shift in peak area towards the shoulder region (Figure 24, blue trace; Table 9).

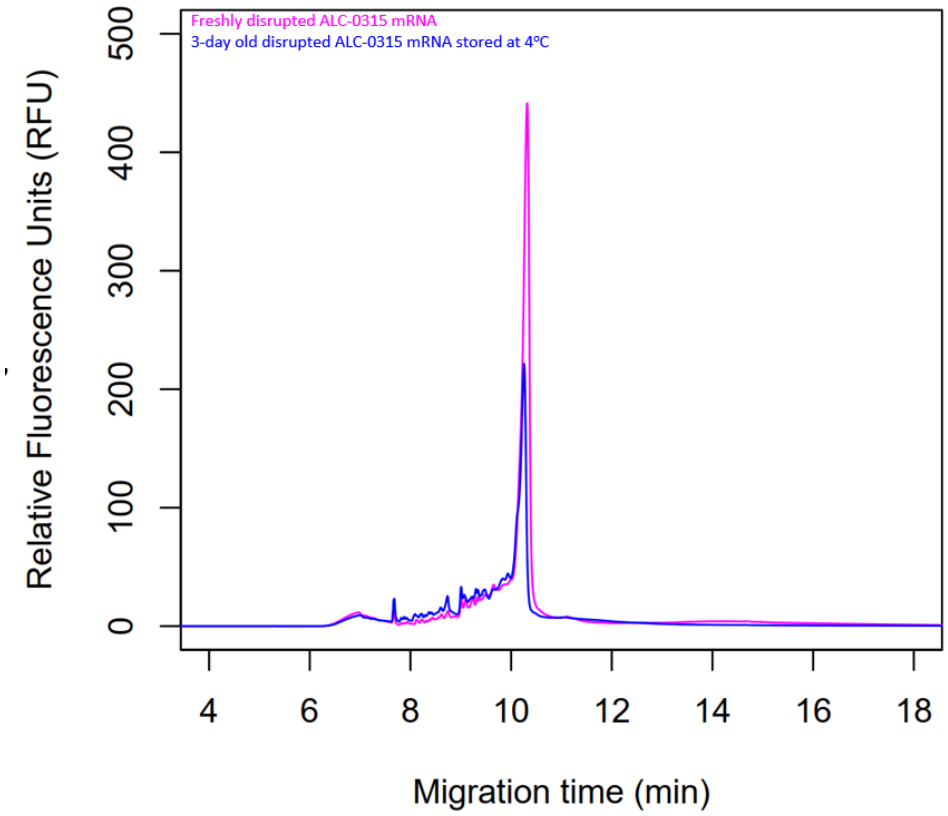

Figure 24. Comparison of FLuc mRNA-LNP after 5 weeks of storage at 4°C (magenta) to the sample FLuc mRNA-LNP sample after 3 days at 4°C but with the LNP disrupted. Analyses were performed in triplicate (n = 3).

Table 9. Area distribution of mRNA-LNP samples by CGE-LIF after LNP disruption. Values were calculated based on the average of triplicates (n = 3).

Sample	% peak area	
	Shoulder	Main peak
FLuc mRNA-LNP stored at 4°C for 5 weeks	44.07	55.93
Disrupted FLuc mRNA-LNP stored at 4°C for 3 days	64.57	35.43

5.3.2 Thermal stability of mRNA extracted from LNP over time

To better understand the conditions under which mRNA degrades following LNP disruption, a thermal stability study was conducted over the course of four weeks. We observed a clear difference in the mRNA profile over the course of five weeks stored at the different temperatures (Figure 25). The sample stored in the -80°C remained quite stable with little shifts in the peak profile and integrity (Table 10). At 4°C and room temperature (RT) storage, the main peak area decreases over time and appears to contribute to the growing shoulder region – degradation is much more significant at RT. To quantify the degradation observed, each trace was integrated to determine the mRNA integrity and monitor the change at the various temperatures and timepoints (Table 10). The profile of the traces appears extremely consistent across all the samples from week to week, regardless of storage temperature. This may suggest that the mechanism of mRNA fragmentation by thermal stress will yield the same products regardless of temperature as long as there is sufficient energy for bond breaking (*64*).

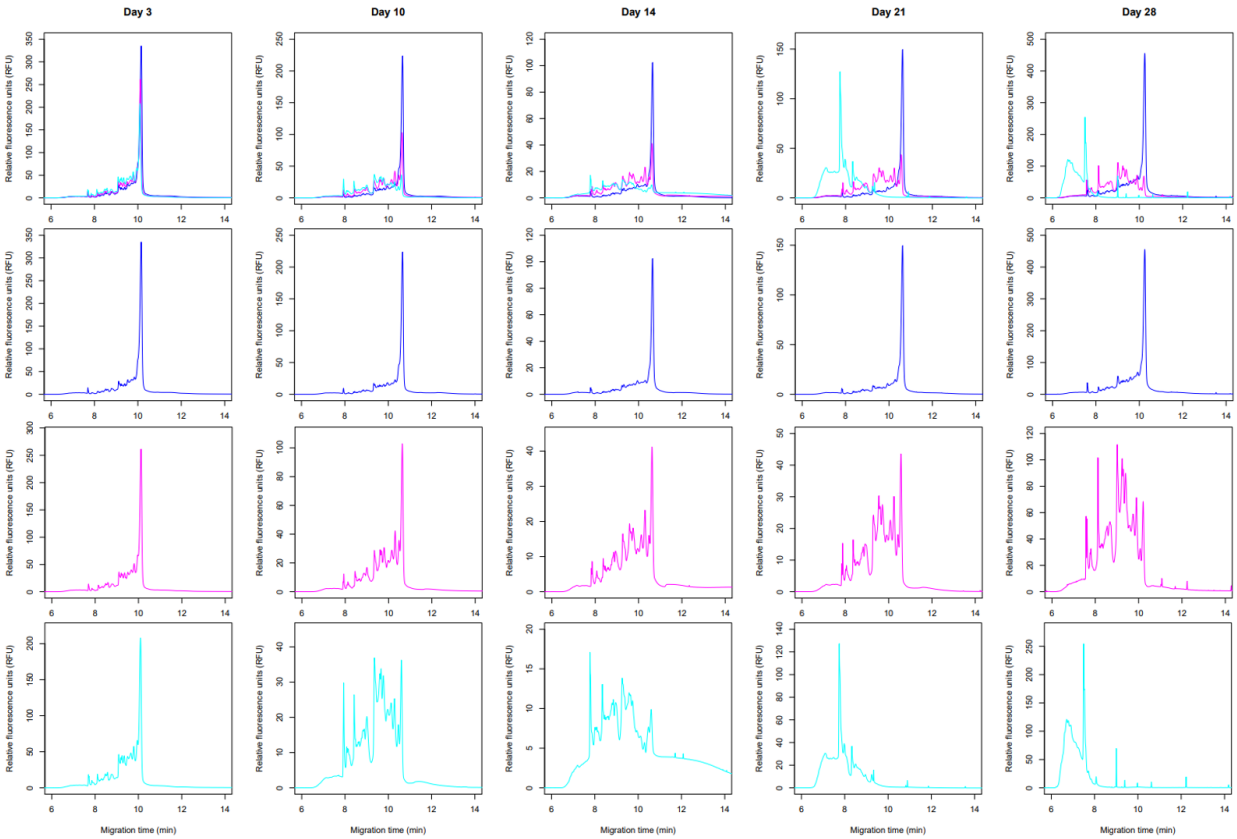

Figure 25. FLuc mRNA profile over four weeks stored at -80°C (second row, dark blue), 4°C (third row, magenta), and RT (fourth row, cyan) after extraction from LNPs, with an overall overlay presented in the first row. Analyses for each sample were performed in triplicate (n = 3).

Table 10. Main peak area (%) of FLuc RNA over the course of four weeks stored at different temperatures after extraction from LNPs. Values were calculated based on the average of triplicates (n = 3).

Storage Condition	% main peak area (%)					
	Day 0	Day 3	Day 10	Day 14	Day 21	Day 28
-80°C		53.94	64.46	57.75	53.96	56.20
4°C		51.08	28.24	27.85	15.31	10.67
RT		35.47	13.04	36.02	N/A	N/A

6 Conclusion

The analysis of mRNA-based products presents significant challenges, as evidenced by inconsistencies in both product integrity and sizing across various separation techniques such as CGE-LIF and IP-RP HPLC. Each method employs unique mechanisms influencing RNA migration and impurity profiles differently; therefore, a comprehensive understanding is necessary to be able to compare products. As it currently stands, integrity measured by CGE-LIF and IP-RP HPLC are not directly comparable out of the box and require careful comparability exercises.

Moreover, the field of mRNA biotherapeutics and its regulation is still in its early stages, necessitating further exploration. Although a foundational understanding is gradually emerging, the analysis and standardization of mRNA quality attributes remain challenging. Despite the development of numerous RNA analysis methods, most were not designed for biotherapeutics. Many existing methods come from research environments; therefore, there is a pressing need to identify parameters in a biotherapeutic context. DOE has proven valuable in probing analytical method parameters by revealing interactions missed in single-factor experiments. Our research shows that mRNA integrity measurements by CGE are highly sensitive to additives, demonstrating the need for further exploration of their effects on therapeutic RNA.

As therapeutics trend toward personalized products, it becomes increasingly difficult to develop specific assays for each individual product. In such cases where bioassays are not feasible or practical, physicochemical assays are relied upon to ensure product quality, safety, and efficacy. This dependence necessitates a focus on developing a strong understanding of analytical techniques and how each component of a therapeutic product

(RNA, excipients etc.) interacts with the analytical system to influence results. As such, we hope that this work will bring more focus on elucidating interactions and mechanisms involved in mRNA analysis and lay the groundwork to establishing clear specifications and regulatory requirements for this product class.

7 References

1. N. Pardi, M. J. Hogan, F. W. Porter, D. Weissman, mRNA vaccines - a new era in vaccinology. *Nat. Rev. Drug Discov.* **17**, 261–279 (2018).

2. S. Qin, X. Tang, Y. Chen, K. Chen, N. Fan, W. Xiao, Q. Zheng, G. Li, Y. Teng, M. Wu, X. Song, mRNA-based therapeutics: powerful and versatile tools to combat diseases. *Signal Transduct. Target. Ther.* **7**, 166 (2022).

3. G. Zhang, T. Tang, Y. Chen, X. Huang, T. Liang, mRNA vaccines in disease prevention and treatment. *Signal Transduct. Target. Ther.* **8**, 1–30 (2023).

4. C. Zhang, G. Maruggi, H. Shan, J. Li, Advances in mRNA Vaccines for Infectious Diseases. *Front. Immunol.* **10** (2019).

5. S. C. Kim, S. S. Sekhon, W.-R. Shin, G. Ahn, B.-K. Cho, J.-Y. Ahn, Y.-H. Kim, Modifications of mRNA vaccine structural elements for improving mRNA stability and translation efficiency. *Mol. Cell. Toxicol.* **18**, 1–8 (2022).

6. R. Verbeke, I. Lentacker, S. C. De Smedt, H. Dewitte, The dawn of mRNA vaccines: The COVID-19 case. *J. Controlled Release* **333**, 511–520 (2021).

7. S. Hossaini, F. Keramat, Z. Cheraghi, B. Zareie, A. Doosti-Irani, Comparing the Efficacy and Adverse Events of Available COVID-19 Vaccines Through Randomized Controlled Trials: Updated Systematic Review and Network Meta-analysis. *J. Res. Health Sci.* **23**, e00593 (2023).

8. E. Dolgin, The tangled history of mRNA vaccines. *Nature* **597**, 318–324 (2021).

9. K. Bloom, F. van den Berg, P. Arbuthnot, Self-amplifying RNA vaccines for infectious diseases. *Gene Ther.* **28**, 117–129 (2021).

10. U. Sahin, K. Karikó, Ö. Türeci, mRNA-based therapeutics — developing a new class of drugs. *Nat. Rev. Drug Discov.* **13**, 759–780 (2014).

11. F. Muttach, N. Muthmann, A. Rentmeister, Synthetic mRNA capping. *Beilstein J. Org. Chem.* **13**, 2819–2832 (2017).

12. A. Ramanathan, G. B. Robb, S.-H. Chan, mRNA capping: biological functions and applications. *Nucleic Acids Res.* **44**, 7511–7526 (2016).

13. A. Shatkin, J. Manley, The ends of the affair: Capping and polyadenylation (2000). https://www-nature-com.proxy.bib.uottawa.ca/articles/nsb1000_838.

14. T. Kawasaki, T. Kawai, Discrimination Between Self and Non-Self-Nucleic Acids by the Innate Immune System. *Int. Rev. Cell Mol. Biol.* **344**, 1–30 (2019).

15. S. Daffis, K. J. Szretter, J. Schriewer, J. Li, S. Youn, J. Errett, T.-Y. Lin, S. Schneller, R. Zust, H. Dong, V. Thiel, G. C. Sen, V. Fensterl, W. B. Klimstra, T. C. Pierson, R. M. Buller, M. Gale Jr, P.-Y. Shi, M. S. Diamond, 2′-O methylation of the viral mRNA cap evades host restriction by IFIT family members. *Nature* **468**, 452–456 (2010).

16. R. Züst, L. Cervantes-Barragan, M. Habjan, R. Maier, B. W. Neuman, J. Ziebuhr, K. J. Szretter, S. C. Baker, W. Barchet, M. S. Diamond, S. G. Siddell, B. Ludewig, V. Thiel, Ribose 2′-O-methylation provides a molecular signature for the distinction of self and non-self mRNA dependent on the RNA sensor Mda5. *Nat. Immunol.* **12**, 137–143 (2011).

17. D. W. Leung, G. K. Amarasinghe, When your cap matters: structural insights into self vs non-self recognition of 5′ RNA by immunomodulatory host proteins. *Curr. Opin. Struct. Biol.* **36**, 133–141 (2016).

18. Cap 1 Messenger RNA Synthesis with Co-transcriptional CleanCap® Analog by In Vitro Transcription - Henderson - 2021 - Current Protocols - Wiley Online Library. https://currentprotocols.onlinelibrary.wiley.com/doi/10.1002/cpz1.39.

19. B. Hornblow, B. Robb, G. Tzertzinis, Mind your caps and Poly A tails | NEB. https://international.neb.com/tools-and-resources/feature-articles/minding-your-caps-and-tails.

20. Understanding COVID-19 mRNA Vaccines, *Genome.gov*. https://www.genome.gov/about-genomics/fact-sheets/Understanding-COVID-19-mRNA-Vaccines.

21. S. S. Rosa, D. M. F. Prazeres, A. M. Azevedo, M. P. C. Marques, mRNA vaccines manufacturing: Challenges and bottlenecks. *Vaccine* **39**, 2190–2200 (2021).

22. I. Knezevic, M. A. Liu, K. Peden, T. Zhou, H.-N. Kang, Development of mRNA Vaccines: Scientific and Regulatory Issues. *Vaccines* **9**, 81 (2021).

23. Frontiers | The Critical Contribution of Pseudouridine to mRNA COVID-19 Vaccines. https://www.frontiersin.org/articles/10.3389/fcell.2021.789427/full.

24. D. Laczkó, M. J. Hogan, S. A. Toulmin, P. Hicks, K. Lederer, B. T. Gaudette, D. Castaño, F. Amanat, H. Muramatsu, T. H. Oguin, A. Ojha, L. Zhang, Z. Mu, R. Parks, T. B. Manzoni, B. Roper, S. Strohmeier, I. Tombácz, L. Arwood, R. Nachbagauer, K. Karikó, J. Greenhouse, L. Pessaint, M. Porto, T. Putman-Taylor, A. Strasbaugh, T.-A. Campbell, P. J. C. Lin, Y. K. Tam, G. D. Sempowski, M. Farzan, H. Choe, K. O. Saunders, B. F. Haynes, H. Andersen, L. C. Eisenlohr, D. Weissman, F. Krammer, P. Bates, D. Allman, M. Locci, N. Pardi, A Single Immunization with Nucleoside-Modified mRNA Vaccines Elicits Strong Cellular and Humoral Immune Responses against SARS-CoV-2 in Mice. *Immunity* **53**, 724-732.e7 (2020).

25. K. D. Nance, J. L. Meier, Modifications in an Emergency: The Role of N1-Methylpseudouridine in COVID-19 Vaccines. *ACS Cent. Sci.* **7**, 748–756 (2021).

26. mRNA Vaccine Process Manufacturing. https://www.sigmaaldrich.com/CA/en/applications/pharmaceutical-and-biopharmaceutical-manufacturing/vaccine-manufacturing/mrna-vaccines-process-manufacturing.

27. J. Whitley, C. Zwolinski, C. Denis, M. Maughan, L. Hayles, D. Clarke, M. Snare, H. Liao, S. Chiou, T. Marmura, H. Zoeller, B. Hudson, J. Peart, M. Johnson, A. Karlsson, Y. Wang, C. Nagle, C. Harris, D. Tonkin, S. Fraser, L. Capiz, C. L. Zeno, Y. Meli, D. Martik, D. A. Ozaki, A. Caparoni, J. E. Dickens, D. Weissman, K. O. Saunders, B. F. Haynes, G. D. Sempowski, T. N. Denny, M. R. Johnson, Development of mRNA manufacturing for vaccines and therapeutics: mRNA platform requirements and development of a scalable production process to support early phase clinical trials. *Transl. Res.* **242**, 38–55 (2022).

28. Health Canada, Good manufacturing practices guide for drug products (GUI-0001) (2018). https://www.canada.ca/en/health-canada/services/drugs-health-products/compliance-enforcement/good-manufacturing-practices/guidance-documents/gmp-guidelines-0001/document.html.

29. X. Xu, T. Xia, Recent Advances in Site-Specific Lipid Nanoparticles for mRNA Delivery. *ACS Nanosci. Au* **3**, 192–203 (2023).

30. X. Zhang, Y. Li, Z. Zhou, Lipid Nanoparticle-Based Delivery System-A Competing Place for mRNA Vaccines. *ACS Omega* **9**, 6219–6234 (2024).

31. R. Cross, Without these lipid shells, there would be no mRNA vaccines for COVID-19. https://cen.acs.org/pharmaceuticals/drug-delivery/Without-lipid-shells-mRNA-vaccines/99/i8.

32. C. Hald Albertsen, J. A. Kulkarni, D. Witzigmann, M. Lind, K. Petersson, J. B. Simonsen, The role of lipid components in lipid nanoparticles for vaccines and gene therapy. *Adv. Drug Deliv. Rev.* **188**, 114416 (2022).

33. M. D. Buschmann, M. J. Carrasco, S. Alishetty, M. Paige, M. G. Alameh, D. Weissman, Nanomaterial Delivery Systems for mRNA Vaccines. *Vaccines* **9**, 65 (2021).

34. A. M. Reichmuth, M. A. Oberli, A. Jaklenec, R. Langer, D. Blankschtein, mRNA vaccine delivery using lipid nanoparticles. *Ther. Deliv.* **7**, 319–334 (2016).

35. USP, Analytical Procedures for mRNA Vaccine Quality Draft Guidelines, 2nd edition.

36. Development of a guideline on the quality aspects of mRNA vaccines - Scientific guideline | European Medicines Agency. https://www.ema.europa.eu/en/development-guideline-quality-aspects-mrna-vaccines-scientific-guideline.

37. K.-W. Wan, F. Galaway, MHRA regulatory considerations for the quality of mRNA products. *Nucleic Acid Insights*, doi: 10.18609/nai.2024.020 (2024).

38. D. S. Dimitrov, Therapeutic Proteins. *Methods Mol. Biol. Clifton NJ* **899**, 1–26 (2012).

39. B. Leader, Q. J. Baca, D. E. Golan, Protein therapeutics: a summary and pharmacological classification. *Nat. Rev. Drug Discov.* **7**, 21–39 (2008).

40. H. Banoun, mRNA: Vaccine or Gene Therapy? The Safety Regulatory Issues. *Int. J. Mol. Sci.* **24**, 10514 (2023).

41. J. Talap, J. Zhao, M. Shen, Z. Song, H. Zhou, Y. Kang, L. Sun, L. Yu, S. Zeng, S. Cai, Recent advances in therapeutic nucleic acids and their analytical methods. *J. Pharm. Biomed. Anal.* **206**, 114368 (2021).

42. A. Demelenne, A.-C. Servais, J. Crommen, M. Fillet, Analytical techniques currently used in the pharmaceutical industry for the quality control of RNA-based therapeutics and ongoing developments. *J. Chromatogr. A* **1651**, 462283 (2021).

43. M. Packer, D. Gyawali, R. Yerabolu, J. Schariter, P. White, A novel mechanism for the loss of mRNA activity in lipid nanoparticle delivery systems. *Nat. Commun.* **12**, 6777 (2021).

44. E. Oude Blenke, E. Örnskov, C. Schöneich, G. A. Nilsson, D. B. Volkin, E. Mastrobattista, Ö. Almarsson, D. J. A. Crommelin, The Storage and In-Use Stability of mRNA Vaccines and Therapeutics: Not A Cold Case. *J. Pharm. Sci.* **112**, 386–403 (2023).

45. C. J. Wilusz, M. Wormington, S. W. Peltz, The cap-to-tail guide to mRNA turnover. *Nat. Rev. Mol. Cell Biol.* **2**, 237–246 (2001).

46. H. K. Patel, K. Zhang, R. Utegg, E. Stephens, S. Salem, H. Welch, S. Grobe, J. Schlereth, A. N. Kuhn, J. Ryczek, D. J. Cirelli, T. F. Lerch, Characterization of BNT162b2 mRNA to Evaluate Risk of Off-Target Antigen Translation. *J. Pharm. Sci.* **112**, 1364–1371 (2023).

47. L. Schoenmaker, D. Witzigmann, J. A. Kulkarni, R. Verbeke, G. Kersten, W. Jiskoot, D. J. A. Crommelin, mRNA-lipid nanoparticle COVID-19 vaccines: Structure and stability. *Int. J. Pharm.* **601**, 120586 (2021).

48. M. A. Liu, T. Zhou, R. L. Sheets, H. Meyer, I. Knezevic, WHO informal consultation on regulatory considerations for evaluation of the quality, safety and efficacy of RNA-based prophylactic vaccines for infectious diseases, 20-22 April 2021. *Emerg. Microbes Infect.* **11**, 384–391 (2022).

49. J. Camperi, S. Lippold, L. Ayalew, B. Roper, S. Shao, E. Freund, A. Nissenbaum, C. Galan, Q. Cao, F. Yang, C. Yu, A. Guilbaud, Comprehensive Impurity Profiling of mRNA: Evaluating Current Technologies and Advanced Analytical Techniques. *Anal. Chem.*, doi: 10.1021/acs.analchem.3c05539 (2024).

50. comirnaty-h-c-5735-x-0044-g-epar-assessment-report-extension_en.pdf. https://www.ema.europa.eu/en/documents/variation-report/comirnaty-h-c-5735-x-0044-g-epar-assessment-report-extension_en.pdf.

51. B. Wei, A. Goyon, K. Zhang, Analysis of therapeutic nucleic acids by capillary electrophoresis. https://doi.org/10.1016/j.jpba.2022.114928.

52. T. Lu, L. J. Klein, S. Ha, R. R. Rustandi, High-Resolution capillary electrophoresis separation of large RNA under non-aqueous conditions. *J. Chromatogr. A* **1618**, 460875 (2020).

53. L. De Scheerder, A. Sparén, G. A. Nilsson, P.-O. Norrby, E. Örnskov, Designing flexible low-viscous sieving media for capillary electrophoresis analysis of ribonucleic acids. *J. Chromatogr. A* **1562**, 108–114 (2018).

54. Z. Li, X. Dou, Y. Ni, K. Sumitomo, Y. Yamaguchi, Acetic acid denaturing pulsed field capillary electrophoresis for RNA separation. *ELECTROPHORESIS* **31**, 3531–3536 (2010).

55. Y.-C. Shih, C.-R. Liao, I.-C. Chung, Y.-S. Chang, P.-L. Chang, Simultaneous separation of five major ribonucleic acids by capillary electrophoresis with laser-induced fluorescence in the presence of electroosmotic flow: Application to the rapid screening of 5S rRNA from ovarian cancer cells. *Anal. Chim. Acta* **847**, 73–79 (2014).

56. A. Azarani, K. H. Hecker, RNA analysis by ion-pair reversed-phase high performance liquid chromatography. *Nucleic Acids Res.* **29**, e7 (2001).

57. S. Fekete, C. Doneanu, B. Addepalli, M. Gaye, J. Nguyen, B. Alden, R. Birdsall, D. Han, G. Isaac, M. Lauber, Challenges and emerging trends in liquid chromatography-based analyses of mRNA pharmaceuticals. *J. Pharm. Biomed. Anal.* **224**, 115174 (2023).

58. H. Lardeux, A. Goyon, K. Zhang, J. M. Nguyen, M. A. Lauber, D. Guillarme, V. D'Atri, The impact of low adsorption surfaces for the analysis of DNA and RNA oligonucleotides. *J. Chromatogr. A* **1677**, 463324 (2022).

59. T. Kuwayama, M. Ozaki, M. Shimotsuma, T. Hirose, Separation of long-stranded RNAs by RP-HPLC using an octadecyl-based column with super-wide pores. *Anal. Sci. Int. J. Jpn. Soc. Anal. Chem.* **39**, 417–425 (2023).

60. A. Lokras, A. Chakravarty, T. Rades, D. Christensen, H. Franzyk, A. Thakur, C. Foged, Simultaneous quantification of multiple RNA cargos co-loaded into nanoparticle-based delivery systems. *Int. J. Pharm.* **626**, 122171 (2022).

61. B. Chen, M. G. Bartlett, Determination of therapeutic oligonucleotides using capillary gel electrophoresis: Determination of oligonucleotides using CE. *Biomed. Chromatogr.* **26**, 409–418 (2012).

62. Y.-W. Lin, T.-C. Chiu, H.-T. Chang, Laser-induced fluorescence technique for DNA and proteins separated by capillary electrophoresis. *J. Chromatogr. B* **793**, 37–48 (2003).

63. M. Youssef, C. Hitti, J. Puppin Chaves Fulber, A. A. Kamen, Enabling mRNA Therapeutics: Current Landscape and Challenges in Manufacturing. *Biomolecules* **13**, 1497 (2023).

64. X. Tong, J. Raffaele, K. Feller, G. Dornadula, J. Devlin, D. Boyd, J. W. Loughney, J. Shanter, R. R. Rustandi, Correlating Stability-Indicating Biochemical and Biophysical Characteristics with In Vitro Cell Potency in mRNA LNP Vaccine. *Vaccines* **12**, 169 (2024).

65. S. S. Nogueira, E. Samaridou, J. Simon, S. Frank, M. Beck-Broichsitter, A. Mehta, Analytical techniques for the characterization of nanoparticles for mRNA delivery. *Eur. J. Pharm. Biopharm.*, 114235 (2024).

66. C. Malburet, A. Carboni, S. Guinamand, H. Naik, S. Fertier-Prizzon, mRNA extraction from lipid nanoparticles. *J. Chromatogr. A* **1714**, 464545 (2024).

67. J. De Vos, K. Morreel, P. Alvarez, H. Vanluchene, R. Vankeirsbilck, P. Sandra, K. Sandra, Evaluation of size-exclusion chromatography, multi-angle light scattering detection and mass photometry for the characterization of mRNA. *J. Chromatogr. A*, 464756 (2024).

68. G. Sanyal, Development of functionally relevant potency assays for monovalent and multivalent vaccines delivered by evolving technologies. *NPJ Vaccines* **7**, 50 (2022).

69. J. Raffaele, J. W. Loughney, R. R. Rustandi, Development of a microchip capillary electrophoresis method for determination of the purity and integrity of mRNA in lipid nanoparticle vaccines. *Electrophoresis* **43**, 1101–1106 (2022).

70. D. A. Warzak, W. A. Pike, K. D. Luttgeharm, Capillary Electrophoresis Methods for determining the IVT mRNA Critical Quality Attributes of Size and Purity. *SLAS Technol.*, doi: 10.1016/j.slast.2023.06.005 (2023).

71. T. Li, M. Malik, H. Yowanto, Method Evaluation for RNA Purity Analysis Using CE-LIF Technology (2019). 10.13140/RG.2.2.24683.77603.

72. RNA 9000 Purity & Integrity Kit For the PA 800 Plus Pharmaceutical Analysis System Application Guide (2023).

73. T. I. Todorov, O. De Carmejane, N. G. Walter, M. D. Morris, Capillary electrophoresis of RNA in dilute and semidilute polymer solutions. *ELECTROPHORESIS* **22**, 2442–2447 (2001).

74. Y. H. Nai, S. M. Powell, M. C. Breadmore, Capillary electrophoretic system of ribonucleic acid molecules. *J. Chromatogr. A* **1267**, 2–9 (2012).

75. V. K. Saarnio, K. Salorinne, V. P. Ruokolainen, J. R. Nilsson, T.-R. Tero, S. Oikarinen, L. M. Wilhelmsson, T. M. Lahtinen, V. S. Marjomäki, Development of functionalized SYBR green II related cyanine dyes for viral RNA detection. *Dyes Pigments* **177**, 108282 (2020).

76. N. Li, A. Nguyen, J. Diedrich, W. Zhong, Separation of miRNA and its methylation products by capillary electrophoresis. *J. Chromatogr. A* **1202**, 220–223 (2008).

77. H. Wätzig, M. Degenhardt, A. Kunkel, Strategies for capillary electrophoresis: method development and validation for pharmaceutical and biological applications. *Electrophoresis* **19**, 2695–2752 (1998).

78. The GLMSELECT Procedure.

79. What Is Design of Experiments (DOE)? | ASQ. https://asq.org/quality-resources/design-of-experiments.

80. J. Laven, D. Senatore, W. K. Wijting, G. de With, The Partitioning of Octyl Phenol Ethoxylate Surfactant between Water and Sunflower Oil. *Open Colloid Sci. J.* **4** (2011).

81. S. H. Kiaie, N. Majidi Zolbanin, A. Ahmadi, R. Bagherifar, H. Valizadeh, F. Kashanchi, R. Jafari, Recent advances in mRNA-LNP therapeutics: immunological and pharmacological aspects. *J. Nanobiotechnology* **20**, 276 (2022).

82. D. F. Driscoll, Lipid nanoparticle–based COVID-19 vaccines: Ensuring pharmaceutical stability, safety, and efficacy. *Am. J. Health. Syst. Pharm.*, zxad221 (2023).

83. F. Cheng, Y. Wang, Y. Bai, Z. Liang, Q. Mao, D. Liu, X. Wu, M. Xu, Research Advances on the Stability of mRNA Vaccines. *Viruses* **15**, 668 (2023).

8 Contributions of Collaborators

Jun Gao generated the DOE sequences, performed statistical analyses, and generated the models.

Mike Wall provided mRNA-LNP samples for analysis.

Michael Johnston’s laboratory provided FLuc RNA encapsulated in various lipid formulations for analysis.

9 Appendices

9.1 Electropherogram integration example

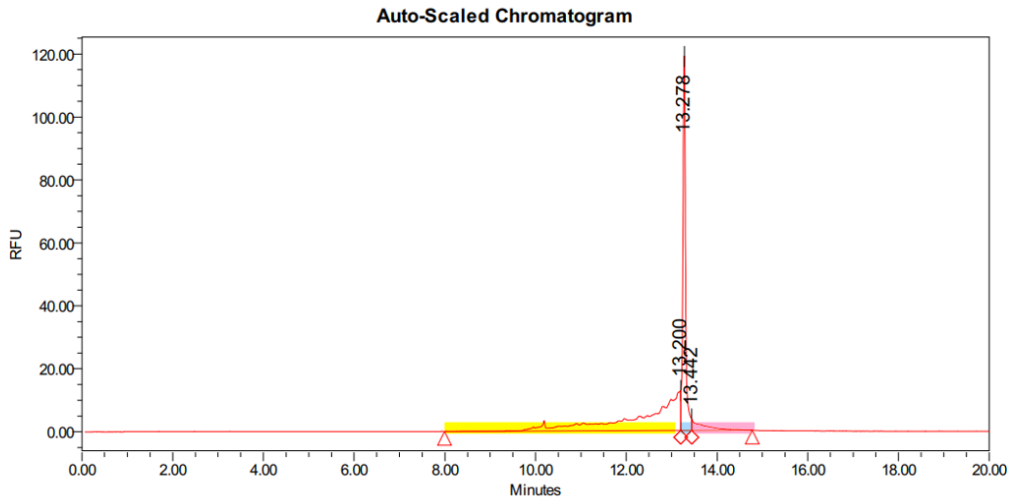

Peak Results

	RT	Area	Height	% Area	Width (sec)	Start Height (µV)	End Height (µV)	Start p/v	End p/v	Width @ Tangent (USP Resolution)
1	13.200	700406766	12632952	55.65	312.500	0	12632952		1.000000	
2	13.278	493874700	119046560	39.24	14.500	12632952	3566495	9.423495	33.379146	9.817697e-002
3	13.442	64222614	3566495	5.10	80.250	3566495	0	1.000000		

Figure A 1. Electropherogram with peak area divided into three parts: shoulder (yellow), main peak (blue), and late-migrating smear (pink).

9.2 Appendix A: Calculation of resolution factor (R_s)

Example calculation for resolution factor between IST and Luciferase RNA analyzed by IP-RP HPLC.

$$R_s = \frac{t_{R2} - t_{R1}}{\frac{1}{2}(W_1 + W_2)}$$

t_{R1} = retention time of first peak

t_{R2} = retention time of second peak

W_1 = width of first peak

W_2 = width of second peak

$$R_s = \frac{14.971\ minutes - 13.833\ minutes}{\frac{1}{2}(36.50\ seconds + 57.65\ seconds)} = \frac{68.28\ seconds}{\frac{1}{2}(94.15\ seconds)} = 1.4504$$